Austrian Journal of Earth Sciences | Vienna | 2016 | Volume 109/2 | 142 - 159 | DOI: 10.17738/ajes.2016.0010

Redox conditions and depositional environment of the Lower Jurassic Bächental bituminous marls (Tyrol, Austria)

Stefan NEUMEISTER[1) *)], Thomas J. ALGEO[2)], Achim BECHTEL[1)], Hans-Jürgen GAWLICK[1)], Reinhard GRATZER[1)] & Reinhard F. SACHSENHOFER[1)]

[1)] Department of Applied Geosciences and Geophysics, Montanuniversitaet Leoben, Peter-Tunner-Str. 5, A-8700 Leoben, Austria;

[2)] Department of Geology, University of Cincinnati, Cincinnati, OH 45221, USA;

[*)] Corresponding author: st.neumeister@hotmail.com

KEYWORDS Sachrang Member; Northern Calcareous Alps; oceanic anoxic event; trace elements; bioproductivity

Abstract

A suite of trace elements (TEs) characterized by an affinity to reducing environments, including molybdenum (Mo), uranium (U), vanadium (V), copper (Cu), and nickel (Ni), were used to investigate secular variations in environmental redox conditions during deposition of the Bächental bituminous marls (Bächentaler Bitumenmergel). These marls, which belong to the Sachrang Member of the Lower Jurassic Middle Allgäu Formation in the Northern Calcareous Alps, are subdivided on the basis of Al-normalized TE concentrations and concentration ratios into three units that correspond to major shifts in depositional redox conditions. The lower and upper units (Units 1 and 3, respectively) were deposited under suboxic to transiently anoxic conditions. The removal of TEs to the sediment was connected to siliciclastic input, diagenetic processes, and organic-matter accumulation in the sediment. In contrast, the middle unit (Unit 2) was characterized by intense anoxia as reflected in strong TE enrichments and peak total organic carbon (TOC) contents up to 13 %. Enrichment of TEs was linked mainly to adsorption onto organic matter in Unit 2, reflecting control of TE enrichment by the availability of an organic substrate. Comparison of inorganic and organic (e.g., pristane/phytane ratio, gammacerane index) geochemical proxies for environmental conditions permits detection of periods with elevated surface-water bioproductivity. A flourishing of algal and planktonic organisms contributed to the significant increase of TOC content at the base of Unit 2. This increase corresponds to the time-equivalent early Toarcian oceanic anoxic event characterized by the global occurrence of organic-rich sediments.

Eine Auswahl an Spurenelementen (Mo, U, V, Cu, Ni), charakterisiert durch ihre Affinität zu reduzierenden Milieus, wurde verwendet um Variationen der vorherrschenden Redoxbedingungen während der Ablagerung der unterjurassischen Bächentaler Bitumenmergel (Sachrang-Member der Mittleren Allgäu-Formation in den Nördlichen Kalkalpen) zu untersuchen. Die Bitumenmergelabfolge wurde auf Basis dieser Spurenelementdaten in drei Einheiten unterteilt. Anorganisch-geochemische Parameter reflektieren wechselnde Umweltbedingungen während der Ablagerung der Bitumenmergel. Der untere und der obere Bereich (Units 1 und 3) der Bächentaler Bitumenmergel wurden unter suboxischen bis teils anoxischen Bedingungen abgelagert. Die Anreicherung der Spurenelemente im Sediment erfolgte durch siliziklastischen Eintrag, diagenetische Prozesse und Akkumulation von organischem Material. Maximalgehalte an Spurenelementen und von organischem Detritus (bis zu 13 %) bestätigen durchgehend anoxische Bedingungen während der Ablagerung des Mittelteils des Profils (Unit 2). Die Fixierung der Spurenelemente im Sediment erfolgte in diesem Bereich ausschließlich durch Adsorption an organischem Material. Folglich war die Verfügbarkeit von organischem Material der limitierende Faktor für die Spurenelementanreicherung. Der Vergleich der anorganisch-geochemischen und organisch-geochemischen (Pristan/Phytan-Verhältnis, Gammaceran Index) Parameter ermöglicht die Identifizierung von Perioden mit erhöhter Bioproduktivität. Demnach hat ein Aufblühen von algalen und planktonischen Organismen zu den signifikant hohen Gehalten an organischem Material an der Basis von Unit 2 beigetragen. Dieses Intervall entspricht dem Zeitraum des ozeanischen anoxischen Ereignisses des Unteren Toarciums, welches durch weltweites Auftreten von organisch-reichen Sedimenten charakterisiert wird.

1. Introduction

The Lower Toarcian is characterized by the global occurrence of marine deposits containing elevated contents of organic matter (OM; e.g., Jenkyns, 1985, 1988; Jenkyns et al., 2002; Pearce et al., 2008). However, the main factors controlling the production and the preservation of OM in these units remain controversial. The Early Jurassic was an interval of climatic warming and major perturbations of the global carbon cycle triggered by massive volcanic eruptions of the Central Atlantic Magmatic Province (CAMP; Marzoli et al., 1999; Whiteside et al., 2007) and the Karroo-Ferrar large igneous province (LIP; Encarnación et al., 1996; Minor and Mukasa, 1997; Svensen et al., 2007, 2012; Sell et al., 2014). Emission of greenhouse gases during these eruptions resulted in "greenhouse Earth" conditions by the early Toarcian (Pálfy and Smith, 2000; Weissert, 2000; Jenkyns, 2003). Attendant climate changes included an acceleration of the hydrological cycle and an increase of continental weathering. These global perturbations induced a flourishing of oceanic bioproductivity caused by an increa-

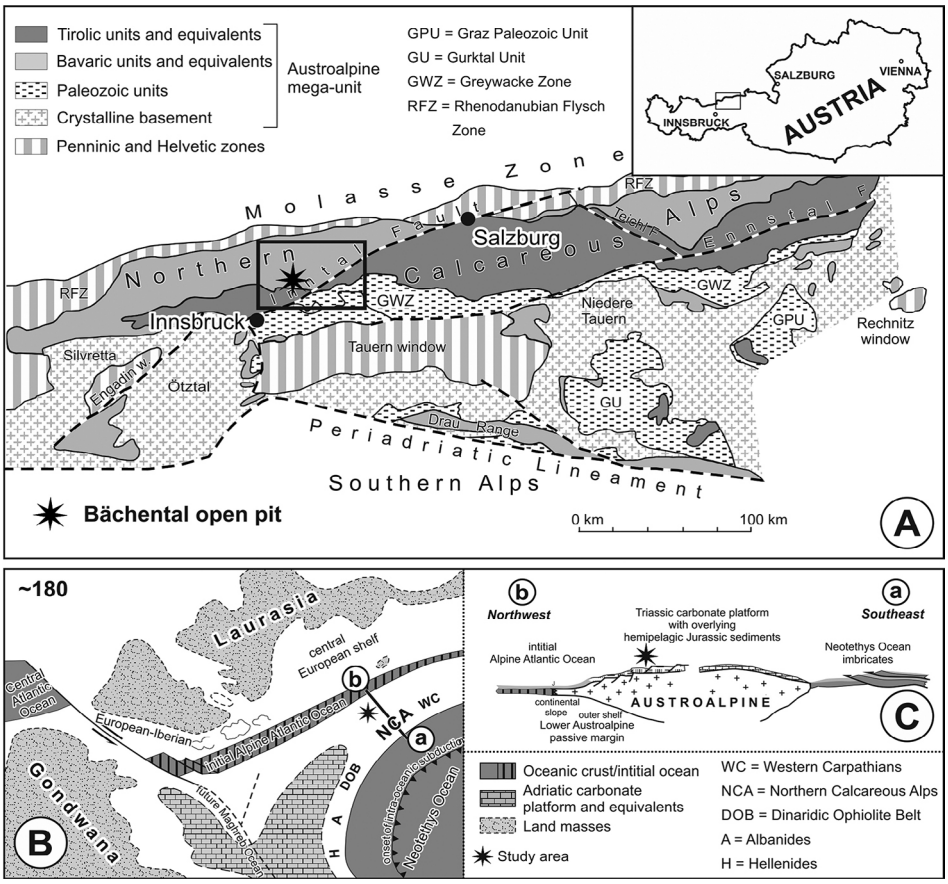

Figure 1: (A) Schematic tectonic map of the Eastern Alps (after Frisch and Gawlick, 2003) with the position of the studied Bächental section. (B) Palaeogeographic position of the study section as part of the Northern Calcareous Alps within the Austroalpine domain in late Early Jurassic time (modified after Gawlick et al., 2009). (C) Schematic cross section (line a-b in B) showing the passive continental margin of the Lower Austroalpine domain (modified after Gawlick et al., 2009). Rifting and spreading of the Alpine Atlantic commencing in the late Early Jurassic affected the Austroalpine domain by the formation of extensional, asymmetric basins exhibiting horst-and-graben structure (cf. Bernoulli and Jenkyns, 1974).

sed supply of nutrients to surface waters as well as the establishment of conditions favoring the development of anoxia and deposition of black shales (Parrish and Curtis, 1982; Parrish, 1993; Cohen et al., 2004). The accumulation of OM-rich deposits has been attributed to (1) upwelling connected with an oceanic anoxic event (T-OAE; Jenkyns, 1985, 1988; see summary in Jenkyns, 2010), (2) a surface-water layer with reduced salinity that caused intensified water-column stratification in epicontinental areas of the western Tethyan realm (Praus and Riegel, 1989; Littke et al., 1991; Sælen et al., 1996), and (3) minor sea-level fluctuations that controlled watermass exchange and, hence, dissolved oxygen levels in semi-restricted basins within the western European epicontinental sea located on the northern side of the Alpine Atlantic (Röhl et al., 2001; Schmid-Röhl et al., 2002; Frimmel et al., 2004). The latter model can also be adapted to the southern side of the Alpine Atlantic, i.e., the "Lower Austroalpine margin" (Figure 1). For any of these mechanisms, short-term variation in OM accumulation may have been modulated by orbital forcings (Ikeda and Hori, 2014).

Redox variation is a key feature of any depositional system that influences the accumulation/formation of OM, TEs, and diagenetic phases. There are several methods for assessing paleoredox variation including organic geochemistry [e.g., pristane/phytane ratio (Pr/Ph), aryl isoprenoids], microscopy (e.g., bioturbation, benthic biofacies), bulk parameters [e.g., relationships between total organic carbon and sulfur (TOC/S), ternary diagram of TOC, iron (Fe), and S], and inorganic geochemical data [e.g., trace element (TE) concentrations, TE ratios]. TEs show low background concentrations only under oxic to weakly suboxic conditions, with authigenic enrichment associated with more reducing conditions (e.g., Piper and Calvert, 2009). This provides the basis for utilization of TE enrichment patterns for paleoredox analysis (e.g., Dean et al., 1999; Tribovillard et al., 2006; Algeo and Tribovillard, 2009). Several of these redox-sensitive elements (including Mo, U, V, Cu, and Ni) show an affinity to anoxic to euxinic paleoenvironments ("euxinic affinity"; e.g., Algeo and Maynard, 2004; Brumsack, 2006; Tribovillard et al., 2006; Piper and Calvert, 2009), as confirmed by TE data from modern euxinic environments (e.g., Dean et al., 1999; Yarincik et al., 2000; Morford et al., 2001).

The Bächentaler Bitumenmergel consists of a 24-m-thick succession of bituminous marls in the Bächental valley of Tyrol in the Northern Calcareous Alps (Figures 1A, 2). Neumeister et al. (2015) investigated controls on OM accumulation in the semi-restricted Bächental basin using a multidisciplinary approach based on microscopy, X-ray diffraction (XRD), bulk geochemistry, stable isotopy, and organic geochemistry. They identified influences on OM accumulation operating on both global (e.g., magmatism, opening of the Alpine Atlantic Ocean) and local scales (e.g., basin morphology, salinity variations). Significant secular variation in TOC (1.1-12.9 %) was induced by paleoenvironmental changes within the Bächental basin, including watermass redox state. Redox variations are clearly reflected by activity of sedimentologic (lamination-bioturbation) and organic geochemical proxies (e.g., Pr/Ph ratios, gammacerane index) in the study section. Neumeister

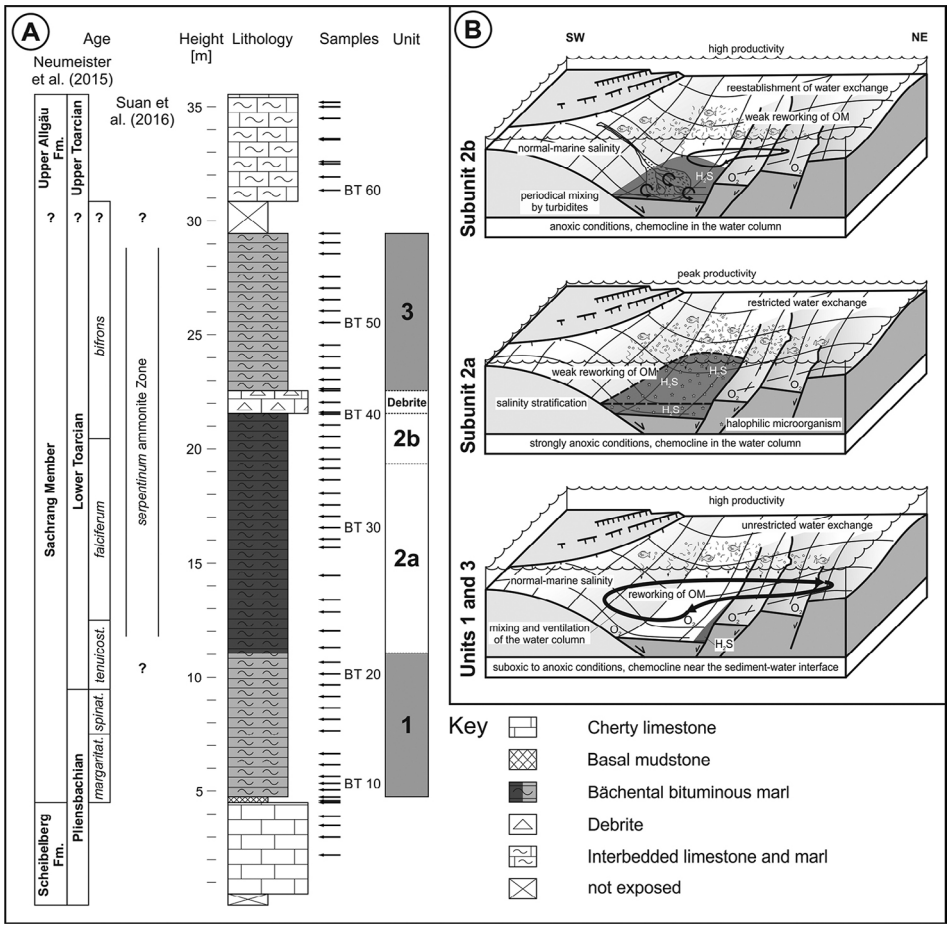

Figure 2: (A) Lithological profile of the investigated Bächental section with positions of samples. Subdivision of the Sachrang Member follow Neumeister et al. (2015). Stratigraphy after Neumeister et al. (2015) and Suan et al. (2016). (B) Depositional environments of the units of the Bächental bituminous marl (after Neumeister et al., 2015). Paleogeographical setting modified after Brandner (2011).

et al. (2015) also established a stratigraphic correlation of time-equivalent OM-enriched sediments between the Alpine realm (i.e., Bächental basin) and western European epicontinental settings.

The Bächentaler Bitumenmergel succession provides an excellent opportunity to compare other proxies such as redox-sensitive TEs with the redox interpretations previously generated on the basis of sedimentologic and organic geochemical data (Neumeister et al., 2015). The goal of the present study, therefore, is to evaluate the utility of multiple redox-sensitive TEs as proxies for watermass redox conditions in a carbonate-dominated basinal setting subjected to a complex set of environmental, depositional, and diagenetic factors. In this study, we focus on the elements Mo, U, V, Cu, and Ni, which are commonly strongly enriched under reducing conditions and generally little affected by post-depositional remobilization (e.g., Tribovillard et al., 2006). Moreover, the application of a suite of TEs provides the possibility for identification of common trends and of irregularities and perturbations possibly related to authigenic uptake of a single TE.

2. Geological setting

The geological setting of the Bächental section, which is well exposed in an open-pit mine, was recently described by Neumeister et al. (2015) and is briefly summarized here. The investigated section is situated in the Bächental valley, which is part of the Karwendel Mountains in western Austria (Figure 1A; GPS: 47°30′31.38″N; 11°37′46.00″E). In this area, lithostratigraphic units of Triassic to Jurassic age belonging to the Lechtal nappe of the Bavaric Unit, a tectonic domain of the Northern Calcareous Alps, are exposed.

In the late Early Jurassic, the study area was situated on the northwestern continental margin of the Neotethys Ocean and the southeastern newly formed passive margin of the Alpine Atlantic (Figures 1B, C). This area was affected by extensional tectonics, related to late Hettangian rifting and Toarcian oceanic break-up in the Alpine Atlantic (Penninic) realm (e.g., Ratschbacher et al., 2004), which resulted in formation of synrift basins such as the Bächental basin. The final configuration of the roughly north-south-trending Bächental basin developed during late Hettangian to Sinemurian time (Schlager and Schöllnberger, 1973). The basin exhibits tilt-block tectonics and antithetic step faults, producing a half-graben geometry with a depocenter in its northern part (Spieler and Brandner, 1989). Deposition of bituminous marls during the early Jurassic was limited to the poorly ventilated deepest part (depocenter) of the Bächental basin (Spieler and Brandner, 1989).

The study section has an overall thickness of ~35 m (Figure 2A). It includes at its base the uppermost 4 m of cherty limestones belonging to the Scheibelberg Formation (Sinemurian to Pliensbachian), which were deposited in water depths of several hundred meters at the transition of distal slope to basin. Overlying the bituminous Middle Allgäu Formation (which includes the Bächentaler Bitumenmergel) is an alternating ~6-m-thick succession of limestone and marl beds belonging to the Upper Allgäu Formation (Spieler and Brandner, 1989).

The Middle Allgäu Formation consists of the 24.90-m-thick Sachrang Member (?late Pliensbachian? to early Toarcian; Tollmann, 1976; Ebli, 1991; Ebli et al., 1998; Gawlick et al., 2009; Neumeister et al., 2015; Suan et al., 2016). The Sachrang

Member is dominated by the Bächental bituminous marls although it also contains a 0.25-m-thick basal mudstone and a 1.00-m-thick debrite layer ~17 m above the base of the unit. The basal mudstone, which consists mainly of quartz and clay minerals of terrigenous origin, marks an abrupt change from nearly pure carbonates to OM-rich marls (Neumeister et al., 2015). The presence of charred organic material and expandable smectite minerals argues for a volcaniclastic contribution to the sediment, which potentially may have triggered the onset of OM accumulation in the Bächental basin (Neumeister et al., 2015). Considerable amounts of smectite are present throughout the Sachrang Member, suggesting continued influx of volcaniclastic material.

The bituminous marl succession was subdivided into three units on the basis of lithology and bulk geochemical data (Figures 2A, B; Neumeister et al., 2015). According to that study, sedimentologic and geochemical proxies indicate mainly suboxic conditions, although with brief periods of anoxia, during deposition of the lowermost unit (Unit 1). This pattern suggests that the chemocline was generally located at shallow depths below the sediment-water interface. The transition to Subunit 2a was characterized by an abrupt shift to strongly anoxic conditions with the chemocline positioned at or above the sediment-water interface. These conditions developed as a consequence of a sea-level lowstand and a subsequent minor sea-level rise, producing a salinity-stratified water column within a stagnant, low-energy basin in which the deep waters became intensely reducing (Neumeister et al., 2015). In this setting, halophilic microorganisms flourished as a consequence of enhanced salinity, and elevated bioproductivity in the surface waters triggered a high sinking flux of OM that supported the establishment and maintenance of anoxic deep-water conditions. A subsequent sea-level rise re-established ventilation of the deep basin and initiated the frequent influx of carbonate turbidites, gradually weakening deep-water anoxia during deposition of Subunit 2b. Finally, a large debris flow effectively ventilated the basin depocenter and permanently re-established suboxic conditions during deposition of Unit 3. Thus, redox and salinity changes in the Bächental basin were determined mainly by sea-level fluctuations that controlled marginal sill depths and the degree of bottom-water ventilation.

The dating of the Bächental bituminous marls to the Toarcian was originally based on the occurrence of *Harpoceras* sp. (Klebelsberg, 1935). This is consistent with the presence of *Cleviceras exaratum* in the middle part of the section, a taxon associated with the early Toarcian *falciferum* Zone (Neumeister et al., 2015). Kodina et al. (1988) inferred that bituminous marl sedimentation began during the late Pliensbachian based on the occurrence of *Arieticeras* sp. and, possibly, *Leptaleoceras* sp. Neumeister et al. (2015) proposed that the deposition of the Sachrang Member in the Bächental basin lasted from late Pliensbachian (*margaritatus* Zone) to early Toarcian (*bifrons* Zone) based on correlation of C_{27}/C_{29} sterane data from Bächental and Dotternhausen (epicontinental Posidonia Shale) sections with sea level. However, new biostratigraphic data – including the reexamination of the ammonites published by Kodina et al. (1988) – indicate that Units 2 and 3 solely belong to the Lower Toarcian *falciferum*-Zone, whereas data for the basal part of the section is missing (Suan et al., 2016). At its type locality in Bavaria, deposition of the Sachrang Member commenced at the base of the *tenuicostatum* Zone and continued through the entire early Toarcian (Ebli et al., 1998).

3. Samples and analytical methods

A total of 62 samples was collected from fresh exposures in a trench that was excavated up to 4 m deep (Figure 2A). This suite includes five samples from the Scheibelberg Formation (BT 2-6), forty-nine samples from the Sachrang Member (BT 7-13, BT 15-26, BT 28-48, BT 50-54, BT 56-58), and nine samples from the lowermost 5 m of the Upper Allgäu Formation (BT 60-68). Note: discontinuous sample numbers owing to a lack of sample material for XRD measurements for samples BT 1, BT 14, BT 27, BT 49, BT 55, and BT 59.

Major- and trace-element concentrations were determined on whole-rock samples using a wavelength-dispersive Rigaku 3040 X-ray fluorescence (XRF) spectrometer in the University of Cincinnati Department of Geology. Raw intensities were calibrated using a set of 65 standards from the USGS, the National Bureau of Standards, and internal lab standards that were analysed by XRAL Incorporated using XRF and INAA. Analytical precision based on replicate analyses was better than ±2 % for major and minor elements and ±5 % for TEs, and detection limits were 1 to 2 ppm for most TEs.

XRD analysis were carried out on bulk samples using Philips X-pert equipment and CuKα-radiation (1.54 Å, 35 kV, 35 mA). The single scans were operated in spin-mode with a goniometer velocity of ½ °/min in the range from 2 to 65° 2θ in the air-dry state (random powder mount). The individual peaks were identified by the use of standardized tables and by comparison with reference samples.

4. Results

In general, all measured TEs (Mo, U, V, Cu, and Ni) show comparable vertical trends (Table 1). TE concentrations are typically low in the TOC-poor samples from the Scheibelberg Formation, the Upper Allgäu Formation, and the debrite layer of the Sachrang Member (Mo: 0.0-2.1 ppm; U: 0.0-1.7 ppm; V: 31-75 ppm; Cu: 0.0-29 ppm; Ni: 0.0-48 ppm). Whereas samples from Units 1 and 3, the basal mudstone, and Subunit 2b feature intermediate TE concentrations (Mo: 0.0-5.5 ppm; U: 0.0-3.5 ppm; V: 43-215 ppm; Cu: 5.9-74 ppm; Ni: 8.3-116 ppm), Subunit 2a is characterized by the highest measured concentrations for all TEs (Mo: 1.1-28 ppm; U: 0.2-3.6 ppm; V: 82-440 ppm; Cu: 28-124 ppm; Ni: 24-64 ppm) except for Ni, which reaches maximum concentrations in the basal mudstone (up to 116 ppm). Peak TE concentrations are generally associated with the TOC-rich lower part of Subunit 2a.

Aluminium (Al) concentrations range between 0.6 % and 6.0 % (Table 1). Carbonate-rich samples from the Scheibel-

Sample	Mo [ppm]	U [ppm]	V [ppm]	Cu [ppm]	Ni [ppm]	Al [%]	Fe [%]	TOC [%]	Mn-rich carbonates [p. a.]	Pr/Ph [conc. ratios]	GI [conc. ratios]
BT 68	1.1	0.7	40.6	4.5	6.2	1.4	0.5	0.1	-	-	-
BT 67	2.1	0.4	65.2	24.0	24.5	4.0	0.9	0.2	-	-	-
BT 66	0.7	1.7	71.5	29.5	48.4	4.9	1.5	0.3	-	-	-
BT 65	B.D.L.	0.9	74.9	28.1	39.5	5.5	1.4	0.3	-	-	-
BT 64	1.5	0.3	31.6	4.8	5.9	1.4	0.4	0.1	-	-	-
BT 63	1.0	0.6	34.2	B.D.L.	B.D.L.	0.6	0.2	0.4	-	-	-
BT 62	1.4	B.D.L.	39.8	5.1	4.2	1.4	0.4	0.1	-	-	-
BT 61	0.8	1.4	64.3	20.9	24.4	4.2	0.9	0.3	-	-	-
BT 60	0.6	1.3	65.9	16.2	25.6	4.3	0.9	0.3	-	-	-
BT 58	3.3	0.4	153.5	73.7	48.4	5.0	4.5	2.8	4990	1.4	0.1
BT 57	3.9	1.8	178.4	73.5	37.3	5.8	4.9	3.0	5080	-	-
BT 56	0.8	0.4	102.1	22.8	12.1	3.0	2.3	2.1	17590	-	-
BT 54	1.8	0.2	43.5	5.9	8.3	2.0	0.5	1.5	17560	-	-
BT 53	0.3	1.5	86.3	13.9	16.1	3.3	3.8	1.6	14040	-	-
BT 52	0.9	0.9	115.7	17.4	16.5	3.4	3.3	1.7	18680	-	-
BT 51	0.4	0.5	84.7	11.1	14.6	2.2	1.7	1.5	21260	-	-
BT 50	0.3	1.5	111.9	12.9	11.8	2.4	2.6	1.6	14960	1.7	0.1
BT 48	0.8	1.8	100.5	21.3	29.6	3.7	2.5	2.1	16510	-	-
BT 47	0.1	1.0	113.2	12.3	14.5	2.6	3.3	1.6	16900	-	-
BT 46	0.3	0.8	101.7	8.6	9.6	2.3	2.5	1.5	15200	-	-
BT 45	0.5	0.7	100.2	13.1	17.5	2.9	3.3	1.5	14100	1.6	0.2
BT 44	0.8	0.1	113.9	15.6	52.2	3.5	4.0	1.9	15990	0.9	0.6
BT 43	0.3	0.7	36.1	3.4	2.4	1.3	0.3	0.1	-	-	-
BT 42	0.8	0.2	31.1	B.D.L.	0.3	0.6	0.2	0.1	-	-	-
BT 41	1.1	0.5	42.2	2.0	3.4	1.2	0.2	0.1	-	-	-
BT 40	1.6	0.3	85.4	30.5	24.5	5.4	2.6	3.0	7830	1.3	0.2
BT 39	1.2	3.5	81.5	35.3	32.3	4.3	3.3	5.6	2630	0.9	0.2
BT 38	4.1	2.5	142.5	45.9	39.4	4.8	3.7	5.6	2690	-	-
BT 37	5.5	2.3	160.2	62.8	45.3	6.0	4.1	6.3	3370	1.1	0.1
BT 36	4.6	0.7	90.6	25.8	20.3	3.2	3.6	2.9	1170	0.9	0.1
BT 35	11.6	3.2	177.6	33.3	38.2	2.7	1.2	9.4	710	0.9	0.8
BT 34	11.1	2.9	217.5	61.3	49.6	3.7	1.6	8.0	2040	-	-
BT 33	1.1	1.4	82.5	40.7	28.8	3.8	1.8	3.6	2430	0.7	0.4
BT 32	4.1	0.7	114.4	37.7	28.5	4.0	5.3	4.0	2400	-	-
BT 31	7.6	2.6	138.2	32.8	29.1	2.6	0.8	5.4	470	0.8	0.6
BT 30	5.1	1.7	172.3	37.3	33.3	3.6	3.1	2.9	2840	0.8	0.3
BT 29	9.5	3.1	187.1	41.7	35.7	2.8	0.9	6.8	740	0.8	0.8
BT 28	3.6	0.2	120.3	27.6	24.2	3.5	4.8	3.5	2520	0.7	0.4
BT 26	9.6	3.6	186.4	53.4	43.9	3.6	1.9	7.6	2830	0.8	0.7
BT 25	27.7	3.6	439.9	123.7	64.1	3.9	2.1	12.9	580	1.0	0.8
BT 24	25.0	3.3	348.2	91.3	56.7	3.3	1.6	11.7	1830	0.9	0.7
BT 23	22.1	1.5	325.1	97.2	50.8	4.1	2.0	9.0	1360	0.8	0.6
BT 22	17.3	1.6	317.4	57.6	52.0	3.6	2.1	8.6	260	0.8	0.8
BT 21	2.9	1.1	174.6	21.7	18.8	3.0	2.4	1.8	13460	-	-
BT 20	1.6	1.1	124.0	22.3	16.1	3.2	2.4	2.0	12720	1.3	0.1
BT 19	2.0	0.8	136.6	48.3	31.6	5.2	4.1	3.3	4280	-	-
BT 18	0.1	1.2	81.1	33.8	28.1	5.6	2.2	2.5	2200	1.4	0.1
BT 17	1.6	0.5	110.8	39.2	26.3	3.4	3.0	1.8	12060	-	-
BT 16	1.1	0.9	128.4	46.9	21.7	4.1	3.0	2.3	11350	-	-
BT 15	B.D.L.	1.2	109.4	36.5	27.4	4.6	3.9	1.9	4940	1.8	0.1
BT 13	0.5	1.4	114.8	14.4	13.2	2.2	6.4	1.1	7750	-	-
BT 12	2.5	3.0	152.6	66.6	34.4	5.3	4.3	2.2	3820	1.0	0.5
BT 11	0.8	0.2	121.1	41.5	28.9	3.9	3.3	1.8	13820	-	-
BT 10	1.6	0.6	120.0	38.9	34.7	4.4	4.0	1.8	13750	1.1	0.4
BT 9	1.0	0.4	120.1	39.5	28.4	4.4	3.7	1.6	12200	-	-
BT 8	2.9	1.0	215.6	66.9	57.2	5.9	8.5	1.6	-	0.9	0.6
BT 7	2.7	B.D.L.	173.5	51.4	115.8	4.4	20.5	1.8	-	-	-
BT 6	0.4	0.4	36.6	0.6	7.9	0.8	0.8	0.1	-	-	-
BT 5	0.7	1.3	37.5	2.2	6.8	0.7	0.2	0.1	-	-	-
BT 4	0.3	0.1	54.1	8.6	15.1	2.7	0.6	0.1	-	-	-
BT 3	0.6	0.5	38.4	5.1	11.2	1.4	0.4	0.1	-	-	-
BT 2	1.4	0.1	42.3	7.4	7.8	1.0	0.3	0.1	-	-	-

Table 1: Geochemical data for samples from the Bächental section.
Notes: Data original to this study except TOC contents, amount of diagenetic Mn-rich carbonates, pristane/phytane ratios (Pr/Ph), and gammacerane index (GI), which are from Neumeister et al. (2015). Stratigraphic units: Scheibelberg Formation, BT 2-6; basal mudstone, BT 7-8; Unit 1, BT 9-21; Subunit 2a, BT 21-35; Subunit 2b, BT 36-40; debrite layer, BT 41-43; Unit 3, BT 44-58; Upper Allgäu Formation, BT 60-68. p.a. = peak area, B.D.L. = below detection limit.

berg Formation, the debrite layer (Sachrang Member) and the Upper Allgäu Formation show the lowest concentrations on average (0.6-2.7 %). In contrast, marls from the Upper Allgäu Formation exhibit high Al concentrations (4.0-5.5 %). Whereas samples from the basal mudstone, Unit 1, and Unit 2 of the Sachrang Member feature Al concentrations in a similar range (2.2-6.0 %), Unit 3 is characterized by low and relatively uniform values (2.0-3.5 %), with elevated values occurring only near its top (up to 5.8 %).

Fe data for the Bächental section, based on a multiple-regression method for intensity-concentration correlation commonly used for shales, was previously published by Neumeister et al. (2015). However, re-assessment of the XRF dataset showed that this standard method is inappropriate for carbonate-rich rock samples containing high amounts of manganese (Mn), such as Bächental bituminous marls, resulting in erroneous absolute elemental concentrations although the vertical trends remain the same. Consequently, the revised Fe data is quoted in Table 1 even though it is not part of the discussion of the present paper.

Results for TOC, Mn-carbonate content, Pr/Ph ratios, and gammacerane index [GI = gammacerane/(gammacerane + αβ C_{30} hopane)] were previously reported by Neumeister et al. (2015). The full geochemical dataset is presented in Table 1.

5. Definitions and models

5.1 Oxygen availability and redox conditions in marine environments

Marine environments show different oxygenation levels depending on setting and water depth. The level of dissolved oxygen in seawater is the basis for classification of environmental redox conditions as oxic (>2 ml O_2 L^{-1}), suboxic (>0 to ~2 ml O_2 L^{-1}), and anoxic (~0 ml O_2 L^{-1}), with measurable quantities of H_2S representing euxinic conditions (Savrda and Bottjer, 1991; Wignall, 1994). These redox states determine the activity of microbially-driven oxidation reactions degrading the OM present in seawater and marine sediments (Breck, 1974).

Oxygen is the dominant electron acceptor that controls the degradation of OM under oxic conditions (Berner, 1981). Under suboxic conditions any remaining oxygen, nitrate, Mn(IV), and Fe(III) serve as electron acceptors (e.g., Tribovillard et al., 2006; Piper and Calvert, 2009). In contrast, sulfate is the dominant electron acceptor under euxinic conditions.

5.2 TEs in marine systems

TEs in oceanic systems derive from two sources: (1) Weathering and erosion of continental crust and subsequent fluvial or atmospheric transport of the products to the global oceans (e.g., Rex and Goldberg, 1958; Martin and Meybeck, 1979) and (2) hydrothermal activity (e.g., Lyle, 1976; Von Damm, 1990). The transport of TEs through the water column as well as their removal to the sediment and their subsequent preservation are mediated by various biogenic and chemical processes in the depositional and diagenetic environments:

(1) TEs transferred with the detrital fraction to the sediment may result in significant concentrations of lithogenously derived TEs (e.g., Dean et al., 1999; Adelson et al., 2001). This process of TE enrichment is especially important for sediments with TOC contents <2.5 % deposited under oxic to suboxic conditions (Algeo and Maynard, 2004; Tribovillard et al., 2006).

(2) Certain dissolved TEs referred to as bio-sensitive (Cu, Ni) are removed from the water column as they participate in marine biogeochemical cycling through assimilatory uptake by planktonic organisms (e.g., Collier and Edmond, 1983; Tribovillard et al., 2006; Piper and Calvert, 2009). The subsequent accumulation of the TE-enriched OM in the sediment contributes to their removal to marine deposits (Ho et al., 2003; Piper and Perkins, 2004; Nameroff et al., 2004; Naimo et al., 2005). The OM-bound fractions of Cu and Ni are liberated by degradation processes and can subsequently be fixed in the sediment through precipitation as Cu- or Ni-sulfide phases or uptake by Fe sulfides provided that anoxic conditions prevail in the burial environment (Huerta-Diaz and Morse, 1992; Achterberg et al., 1997; Morse and Luther, 1999). Hence, high primary productivity is favourable for elevated Cu and Ni concentrations in the sediment (Lewan and Maynard, 1982; Brumsack, 1986; Algeo and Maynard, 2004).

(3) Besides the bio-sensitive Cu and Ni, several other TEs (including Mo, U and V) show an affinity to reducing environments (e.g., Wignall, 1994; Algeo and Maynard, 2004). The accumulation of TEs in the sediment under reducing conditions mainly occurs via chemically-controlled, non-biogenic processes including adsorption onto organic or lithogenic substrates (Mo, V, Ni; e.g., Brumsack, 1989; Morford and Emerson, 1999; Algeo and Maynard, 2004), formation of organometallic ligands (U, V, Cu; e.g., Emerson and Huested, 1991; Morford and Emerson, 1999; Algeo and Maynard, 2004), uptake by authigenic Fe sulfides in solid solution (Mo, Cu, Ni; e.g., Huerta-Diaz and Morse, 1992; Morse and Luther, 1999; Adelson et al., 2001), precipitation as individual solid oxide, hydroxide or sulfide phases (U, V, Cu; e.g., Achterberg et al., 1997; Morse and Luther, 1999; Zheng et al., 2002), and adsorption onto particulate Mn/Fe oxyhydroxides that promote the delivery of TEs to the sediment via redox cycling of Mn and Fe in the water column (Mo, V, Cu, Ni; Adelson et al., 2001; Algeo and Maynard, 2004; Algeo and Tribovillard, 2009). In contrast to the bio-sensitive TEs, enrichment of Mo, U, and V exclusively reflects the prevailing redox conditions during deposition (e.g., Tribovillard et al., 2006).

(4) Remobilization and translocation of TEs during diagenesis can influence TE concentrations in the sediment resulting in TE compositions that do not reflect primary depositional controls (e.g., Breit and Wanty, 1991; Thomson et al., 1993).

5.3 TE-based paleoredox proxies

The classification of TEs in terms of their origin is commonly established via model approaches based on bulk parameters providing estimates of the TE fractions that are derived from either lithogenous or seawater sources (e.g., Calvert and Pe-

dersen, 2007; Perkins et al., 2008; Piper and Calvert, 2009). In this process, the concentration of the TE in question is normalized to a lithogenic element in the sediment (Calvert and Pedersen, 2007; Piper and Calvert, 2009). The use of Al as a normalizing element is common owing to its high concentration in many sediments and its relative immobility in the diagenetic environment (e.g., Wedepohl, 1995; Taylor and McLennan, 1985). The lithogenous fraction of a given TE is commonly estimated based on its relationship to Al: a line is drawn from the origin of the TE-Al crossplot through the sample points with lowest TE concentrations to represent the approximate TE/Al ratio of the lithogenous fraction (e.g., Piper and Calvert, 2009). TE concentrations plotting above this line represent the fractions originating from either biogenous or hydrogenous sources (Piper et al., 2007; Piper and Calvert, 2009).

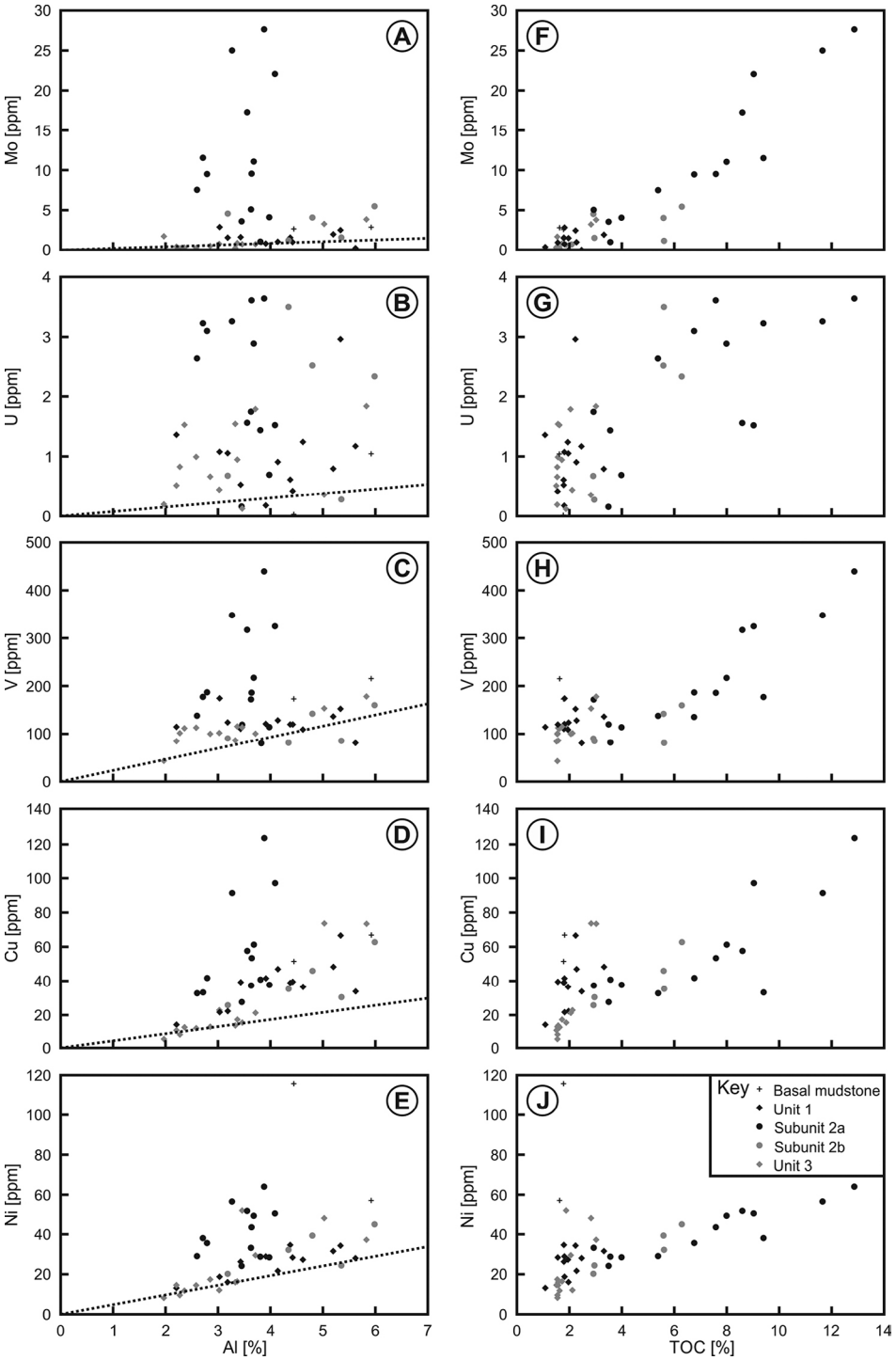

Figure 3: Left: Aluminum (Al) vs. trace element (TE) concentrations: (A) molybdenum (Mo), (B) uranium (U), (C) vanadium (V), (D) copper (Cu), and (E) nickel (Ni). Dotted lines indicate the lithogenous TE fractions, and excess TE concentrations above these lines represent the biogenic and authigenic fractions. Right: Total organic carbon (TOC) vs. TE concentrations: (F) molybdenum (Mo), (G) uranium (U), (H) vanadium (V), (I) copper (Cu), and (J) nickel (Ni). Positive covariation reveals the dependence of TE uptake on organic-matter accumulation.

However, the classification of TE sources by means of this approach entails some limitations and uncertainties:

(1) The removal of TEs by post-depositional alteration processes (e.g., Breit and Wanty, 1991; Thomson et al., 1993) induces a shift to lower TE concentrations that depends on the magnitude of depletion. As a result, this procedure may result in underestimation of lithogenously derived TEs and overestimation of TEs derived from other sources.

(2) Different types of clay minerals can be characterized by varying amounts of mineral-bound TEs (e.g., Wedepohl, 1971; Kogel and Lewis, 2001). Hence, the use of a single detrital TE-Al regression for all samples may produce biased results, if the mineralogical composition of the clay fraction changes during deposition of a section.

(3) This approach presupposes that all non-seawater-derived TEs are bound to the detrital siliciclastic fraction (e.g., Piper and Calvert, 2009). However, lithogenously derived TEs (e.g., Mo, V) can also be incorporated into diagenetic carbonates (see Section 6.2).

(4) Relative amounts of TEs linked to siliciclastics and organics cannot be resolved in sections where Al concentrations and TOC contents show a positive correlation (see Section 6.2).

Despite these limitations, TE-Al diagrams provide a simple method to approximately differentiate TE sources and, therefore, are used in this study (Figures 3A-E).

Plots of TE vs. TOC content (Figures 3F-J) provide additional information about environmental redox conditions and TE removal to the sediment. Linear TE-TOC correlations have been reported from numerous black shale formations (e.g., Holland, 1984; Robl and Barron, 1987; Algeo and Maynard, 2004). According to Algeo and Maynard (2004), TE/TOC relationships depend on redox conditions and TOC thresholds:

(1) There is only little covariation visible in black shales with relatively low TOC contents (<2.5 %) deposited under dysoxic conditions as in that case TEs are mainly connected with the detrital fraction of the sediment.

(2) TEs are mainly present in organometallic complexes under non-sulfidic anoxic conditions (Pratt and Davis, 1992) and, hence, show a significant covariation with TOC content. OM is the limiting factor for TE accumulation in the sediment.

(3) Under euxinic conditions (free H_2S in the water column) the accumulation of TEs is linked to the precipitation of authigenic solid TE phases (e.g., Morse and Luther, 1999) or conversion of reduced TEs to particle-active phases (e.g., Helz et al., 1996), resulting in strong TE enrichment and weak TE-TOC covariation.

However, in stagnant and anoxic settings, TE/TOC ratios may also be affected by the degree of restriction of the subchemoclinal watermass and temporal changes thereof related to deepwater renewal in anoxic basins (Algeo and Lyons, 2006; Algeo and Maynard, 2008; Algeo and Rowe, 2012). In such systems, increasing restriction is reflected by a systematic decrease of TE/TOC ratios in silled basins. This relationship is caused by the continuous depletion of a given TE due to the removal of the element to the sediment without adequate resupply by deepwater renewal ("basin-reservoir effect"; Algeo and Lyons, 2006). Hence, low sedimentary TE concentrations and TE/TOC ratios may reflect significant restriction of silled marine basins. However, it is also possible that, in deep-time systems, low TE concentrations in the sediment reflect low TE concentrations in contemporaneous global seawater (Scott et al., 2008).

The concentrations of authigenic (auth) Mo and U in the sediment can be used to differentiate depositional redox conditions and processes (Algeo and Tribovillard, 2009). According to this study, $(Mo/U)_{auth}$ ratios less than the Mo/U molar ratio of seawater (~7.5-7.9; Chen et al., 1986) typically occur in oceanic systems under suboxic conditions, whereas increasingly reducing and at least occasionally euxinic conditions are reflected by $(Mo/U)_{auth}$ ratios equaling or even exceeding that of seawater. The use of this approach requires the calculation of "enrichment factors" (EF; $X_{EF} = [(X/Al)_{sample}/(X/Al)_{UCC}]$), where X is the element of interest (Tribovillard et al., 2006). For the present study, samples were normalized to the upper continental crust (UCC) compositions of McLennan (2001). The results for Mo_{EF}/U_{EF} ratios for Bächental bituminous marls were plotted in Figure 5 (see Section 6 for discussion).

5.4 Organic geochemical-based paleoredox and -salinity proxies

Stratigraphic variations in redox and salinity conditions during deposition of the Bächental section were determined on the basis of the pristane/phytane (Pr/Ph) ratio and the gammacerane index (GI, hopane isomerization ratio, 4-methylsteranes), respectively (Neumeister et al., 2015). The Pr/Ph ratio is commonly used as a redox indicator during early diagenesis, with values <1.0 indicating anoxic conditions and values >1.0 indicating suboxic to oxic conditions (Didyk et al., 1978). High values for GI indicate a stratified water column in marine and non-marine source-rock depositional environments, commonly resulting from a deep hypersaline water body (Fu et al., 1986). Alternatively, gammacerane may also originate from bacterivorous ciliates floating at the chemocline within the water column (Sinninghe Damsté et al., 1995; Schwark et al., 1998). According to these studies, elevated amounts of gammacerane might reflect a well-stratified water column, even in the absence of high-salinity bottom waters. Furthermore, increased hopane isomerization ratios, which result from diagenetic processes specific for hypersaline conditions (ten Haven et al., 1987), as well as large amounts of 4-methylsteranes, which are frequently related to halophilic microorganisms (e.g., ten Haven et al., 1985), are indicators for an elevated salinity of bottom-waters in the Bächental basin.

6. Discussion

Interpretation of TE concentrations and concentration ratios (TE/Al, TE/TOC) provides information about siliciclastic input, biogenic supply to the basin floor, prevailing redox conditions, and the impact of diagenetic processes. In the following,

		Mo/Al	U/Al	V/Al	Cu/Al	Ni/Al
Upper Allgäu Formation		0.5	0.3	16.5	3.8	5.9
Sachrang Member	**Unit 3**	0.2	0.3	33.7	5.0	5.6
	Debrite layer	0.9	0.5	36.5	1.7	1.8
	Subunit 2b	0.9	0.4	26.7	8.1	7.4
	Subunit 2a	3.0	0.8	59.0	14.7	12.4
	Unit 1	0.3	0.2	29.8	8.9	6.1
	Basal mudstone	0.5	0.1	37.7	11.4	17.9
Scheibelberg Formation		0.5	0.3	40.6	3.2	8.1
Average upper continental crust		0.2	0.3	13.3	3.1	5.5

Table 2: Median TE/Al ratios for stratigraphic units of the Bächental section.
Notes: Values for average upper continental crust are from McLennan (2001).

each stratigraphic unit of the Bächental section is discussed separately.

6.1 TE redox proxies in the Scheibelberg and Upper Allgäu formations

Low TOC contents (<0.5 %) and substantial bioturbation suggest oxic conditions during deposition of limestones and marls of the Scheibelberg and Upper Allgäu formations (Neumeister et al., 2015). This is confirmed by generally low concentrations of Mo, U, V, Cu, and Ni (Figures 4A-E) as well as pronounced positive covariation of all TEs with Al indicating solely lithogenous TE sources for those units. All samples display nearly equal values for Mo/Al, U/Al, Cu/Al, and Ni/Al ratios suggesting a similar siliciclastic source (Table 2). In contrast, the fraction of Al-bound V is significantly higher in the Scheibelberg Formation compared to the Upper Allgäu Formation (Table 2). Comparison of TE/Al ratios for the Upper Allgäu Formation with those for average upper continental crust (McLennan, 2001; Table 2) shows that TE concentrations are close to crustal values. In contrast, samples from the Scheibelberg Formation feature relative enrichment of V and Ni, whereas Mo, U, and Cu concentrations are close to crustal values. Because strong positive TE-Al covariation in both units confirms a dominantly lithogenous source, the differences in TE patterns between the Scheibelberg and Upper Allgäu formations indicate somewhat different sources of detrital material.

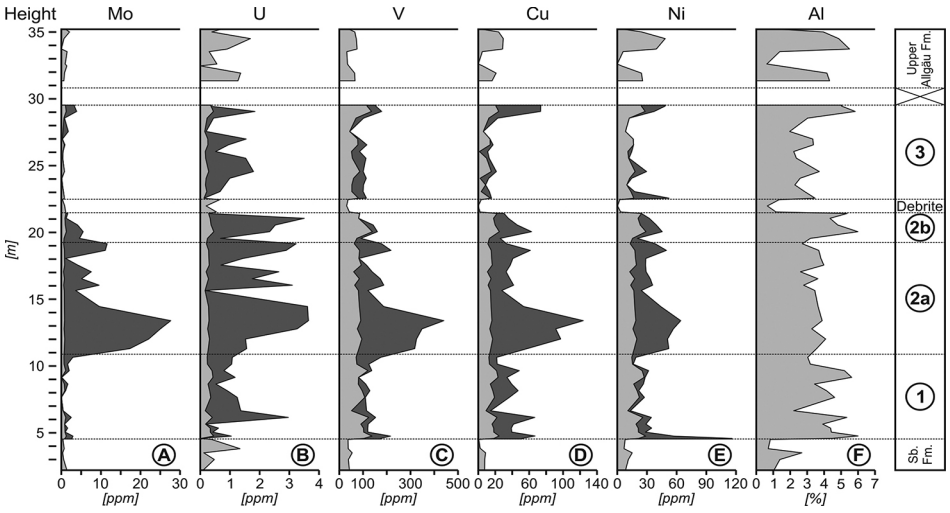

Figure 4: Stratigraphic variation of lithogenous (light grey) and authigenic (dark grey) trace element fractions in the study section: (A) molybdenum (Mo), (B) uranium (U), (C) vanadium (V), (D) copper (Cu), (E) nickel (Ni), and (F) aluminum (Al). Sb. Fm. = Scheibelberg Formation.

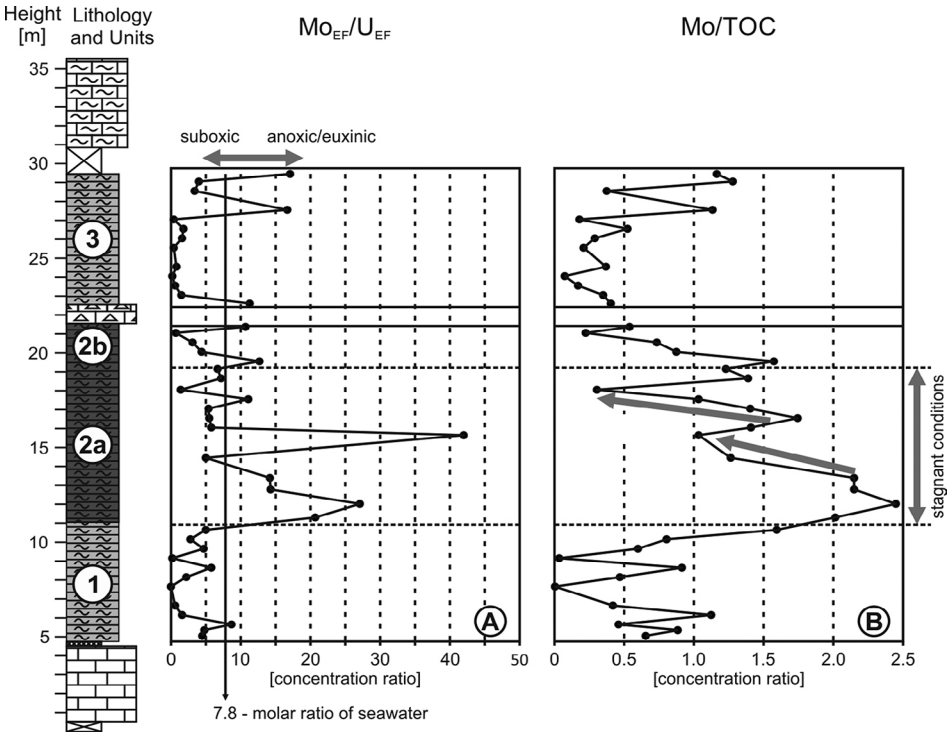

Figure 5: Stratigraphic variation of (A) molybdenum vs. uranium enrichment factor (Mo_{EF}/U_{EF}) and (B) molybdenum vs. total organic carbon (Mo/TOC) ratio. Comparison of Mo/U ratio with that of seawater (~7.8; Chen et al., 1986) provides information about prevailing redox conditions during deposition (Algeo and Tribovillard, 2009). Accordingly, low values of samples from Units 1 and 3 indicate suboxic conditions, whereas elevated values of samples from Unit 2 imply predominating anoxia. Given anoxic conditions, Mo/TOC ratios reflect paleohydrographic restriction (Algeo and Lyons, 2006), with ratios of <3 as for Subunit 2a implying strongly reducing conditions.

6.2 TE redox proxies in the basal mudstone, Unit 1, and Unit 3 of the Sachrang Member

The lower (basal mudstone and Unit 1) and the upper (Unit 3) intervals of the OM-enriched Sachrang Member were deposited under similar environmental conditions. According to geochemical proxies (Pr/Ph, TOC-Fe-S, GI, hopane isomerization ratio, 4-methylsteranes), suboxic conditions and a watermass of normal salinity existed during deposition of these units (Neumeister et al., 2015).

TEs show similar characteristics in the basal mudstone as well as in Units 1 and 3 (Figures 3A-J, 4A-E, 5, 6). Median values for TE/Al ratios are typically in the same range for Units 1 and 3

(Table 2). Mo, U, and Ni show concentrations similar to average upper continental crust, V and Cu concentrations are elevated in both units with higher values occurring in Unit 1 (McLennan, 2001; Table 2). In contrast to the Scheibelberg and Upper Allgäu formations, in which the clay fractions contain only illite, significant amounts of smectite are present in the Bächental bituminous marls. These large amounts of smectite are likely to have been derived from alteration of volcanic ash, indicating a pronounced contribution of volcanic detritus during marl deposition (Neumeister et al., 2015). Thus, it seems likely that the lithogenous TE fractions were related to volcaniclastic inputs to the Sachrang Member. However, differences in clay mineral composition do not markedly influence the fractions of lithogenous-derived TEs in the study section. This is indicated by the similar ranges of TE/Al ratios for samples from the transition zones (i.e., Scheibelberg Formation - basal mudstone and Unit 1 of the Sachrang Member; Unit 3 of the Sachrang Member - Upper Allgäu Formation; Table 2).

The different TEs show varying affinities to siliciclastics, carbonates, and OM in Units 1 and 3 (Figures 4A-J, 6). Positive U-Al covariation suggests that U concentrations were mainly linked to lithogenous inputs. In contrast, Mo and V concentrations show correlations to both Al content and the amount of diagenetic Mn-rich carbonates. Cu and, in part, Ni show vertical trends that are similar to those of Al and TOC (Figure 6). Because samples of Units 1 and 3 are characterized by positive covariation between Al and TOC (Figure 6), it is impossible to determine conclusively whether Cu and Ni enrichment was mainly connected to detrital input or OM accumulation (see Section 5.3). Generally, the removal of Cu and Ni to the sediment is typically controlled by similar processes (e.g., Tribovillard et al., 2006). Besides lithogenous inputs, the main source of the bio-sensitive TEs Cu and Ni to the sediment is adsorption onto OM (Tribovillard et al., 2006). Whereas the latter process is significant in anoxic environments, Cu and Ni is typically connected with the detrital fraction in sediments with moderate TOC content (<2-3 %) deposited under oxic to dysoxic conditions, such as in Units 1 and 3 (TOC: 1.1-3.3 %). However, both bulk geochemical and organic geochemical parameters indicate transient shifts to more reducing conditions during deposition of these units (Neumeister et al., 2015), suggesting that Cu and Ni concentrations were at least partly controlled by adsorption onto OM.

Al concentrations and amount of Mn-rich carbonates show a negative correlation caused by the interrelation of siliciclastic input and carbonate dilution in Units 1 and 3 (Figure 6). In those units, rather constant values for absolute concentrations and TE/Al ratios as well as prevailing suboxic conditions indicate a common source and an accumulation linked to lithogenous inputs for both Mo and V (Figures 4A, C, 6, Table 2). However, Mo and V are characterized by a varying correlation with Al concentrations and amount of Mn-rich carbonates in Units 1 and 3 (Figure 6), indicating that, the uptake of those TEs was related, in different stratigraphic intervals, to either siliciclastics or formation of diagenetic Mn-rich carbonates. Mo and V concentrations reflect primarily detrital inputs in the lower part of Unit 1 (up to sample BT 13, 6.65 m). In contrast, the covariation of Mo and V concentrations with amount of Mn-rich carbonates implies that their enrichment was mainly associated with precipitation of diagenetic Mn-rich carbonates in the upper part of Unit 1 and in parts of Unit 3 (Mo: BT 52-54, 26.55-27.55 m; V: BT 44-50, 22.60-25.55 m; Figure 6). Hence, although Mo and V probably derived from a common lithogenous source, their enrichment in the sediment potentially was controlled by different processes. The occurrence of diagenetic Mn-rich carbonates implies that the sediment accumulated in oxygenated bottom waters (e.g., Calvert and Pedersen, 1996). Apart from the lithogenous contribution, the fixation of the redox-sensitive TEs Mo and V in the sediment requires reducing depositional conditions (e.g., Tribovillard et al., 2006; Piper and Calvert, 2009). Mo and V enrichment under oxic conditions is effected by adsorption onto the surfaces of Mn oxides rather than by reduction (e.g., Algeo and Maynard, 2004; Morford et al., 2005; Tribovillard et al., 2006). However, the absence of corresponding peaks in XRD diffractograms excludes the presence of Mn oxides in bituminous marls of Units 1 and 3 (Neumeister et al., 2015). Dissolution of Mn oxides in sediment layers below the chemocline releases ^{12}C-enriched carbon, Mn, Mo, and V to porewaters (e.g., Morford et al., 2005). Elevated concentrations of Mo und V in porewaters of recent bottom sediments are commonly due to complexation of those elements with dissolved organic carbon (e.g., Emerson and Huested, 1991; Morford et al., 2005). Diagenetic Mn-rich carbonates in samples from Units 1 and 3 contain high amounts of ^{12}C-enriched carbon (Neumeister et al., 2015). Hence, we speculate that the positive covariation among diagenetic Mn-rich carbonates, Mo, and V concentrations in parts of Units 1 and 3 was caused by the incorporation of organic-derived carbon and also its absorbed Mo and V, into the lattice of Mn-rich carbonates during their early diagenetic formation at the chemocline in the sediment.

Bituminous marls from Units 1 and 3 generally feature lower values for Mo_{EF}/U_{EF} ratios (median: 2.2; Figures 5A) relative to the typical Mo/U molar ratio of seawater (~7.8; Chen et al., 1986), which is consistent with suboxic depositional conditions (cf. Algeo and Tribovillard, 2009). However, elevated values, equaling or even exceeding that of seawater, suggest the occurrence of more intensely reducing conditions at the top of Unit 3. Prevailing suboxic conditions and unrestricted deepwater exchange during deposition of Units 1 and 3 (Neumeister et al., 2015) exclude the use of Mo/TOC ratios for interpretation of environmental conditions in those intervals (cf. Algeo and Lyons, 2006).

The debrite at the base of Unit 3 represents a rapidly deposited sediment layer that interrupted bituminous marl sedimentation in the Bächental basin. The low TE concentrations of these OM-poor carbonates are indicative of oxic depositional conditions.

To sum up, the onset of OM accumulation in the Bächental basin was accompanied by a mineralogical change of the clay

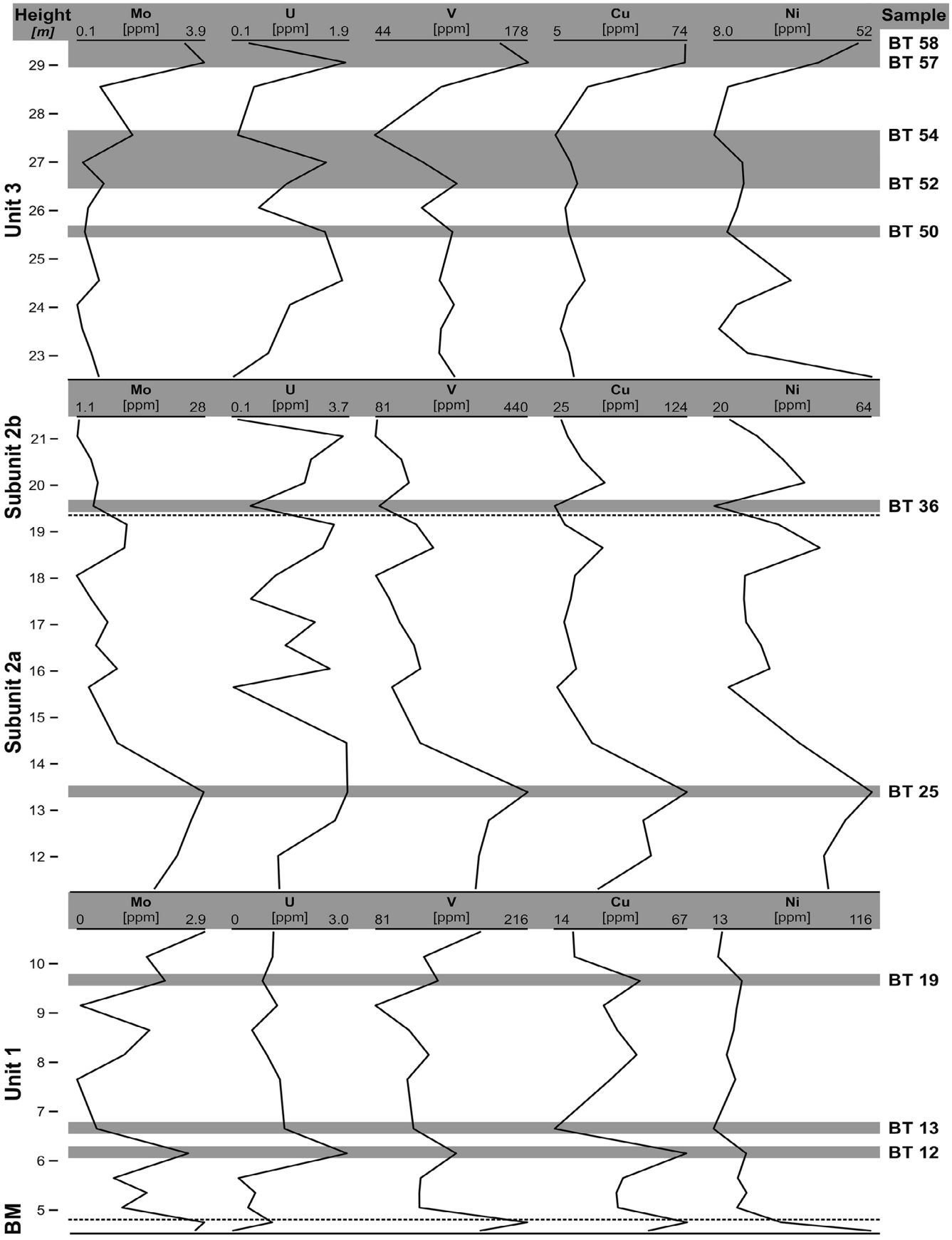

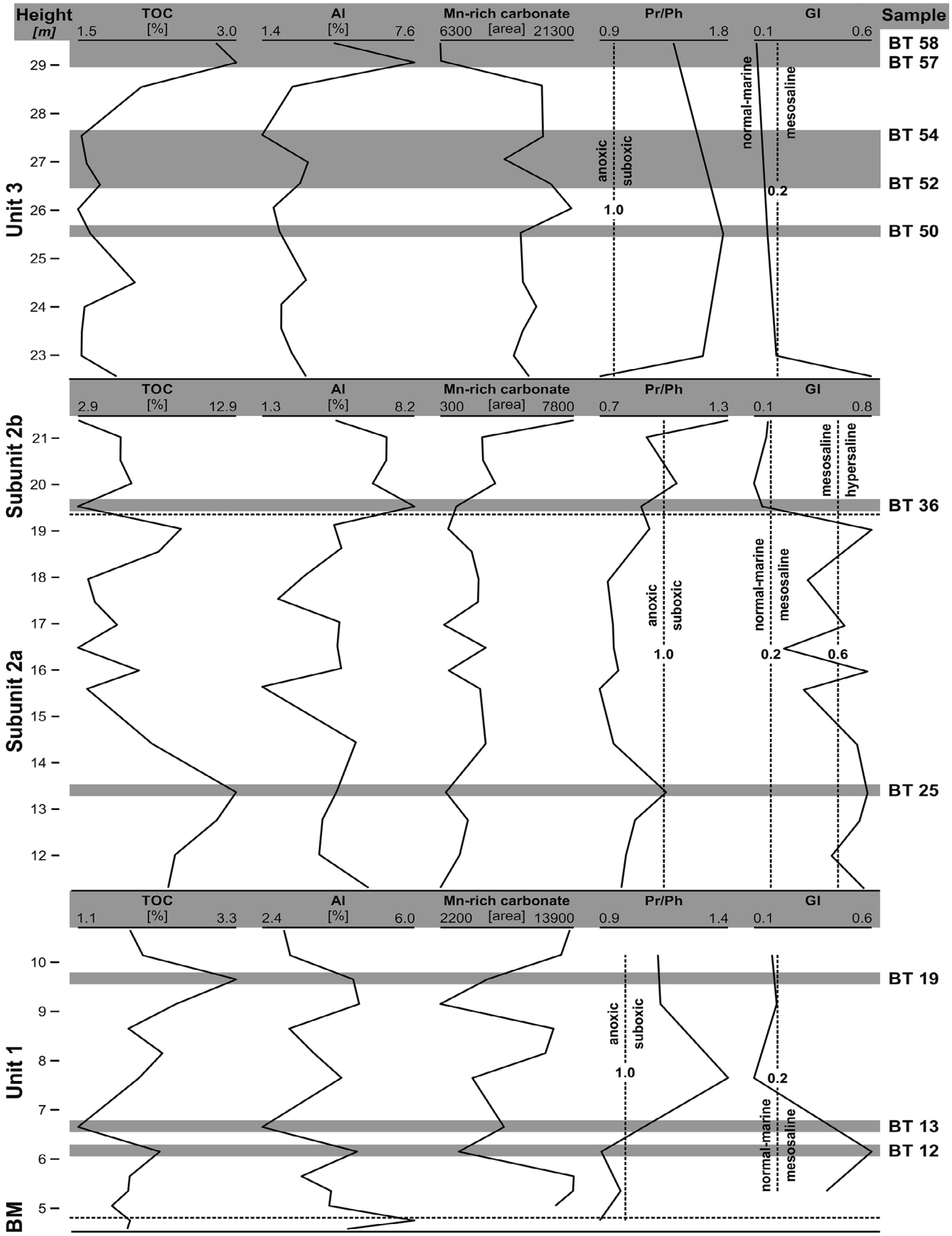

Figure 6: Left: Stratigraphic variation of trace element concentrations: molybdenum (Mo), uranium (U), vanadium (V), copper (Cu), and nickel (Ni). Right: Stratigraphic variation of total organic carbon (TOC), aluminum (Al), amount of diagenetic Mn-rich carbonates, pristane/phytane (Pr/Ph) ratios, and gammacerane index (GI). Note the different scales for the individual units. Relationship between oxic/suboxic and anoxic conditions for Pr/Ph ratios after Didyk et al. (1978). Relationship between salinity conditions and GI after Schwark et al. (1998). Samples characterized by specific attributes are highlighted. See text for explanations.

fraction potentially linked to the onset of volcaniclastic inputs to the sediment. In contrast to U, which was solely derived from lithogenous sources, Mo and V concentrations are characterized by varying relationships to siliciclastic inputs and potentially to precipitation of diagenetic Mn-rich carbonates. Removal of the bio-sensitive elements Cu and Ni to the sediment was established by means of adsorption onto OM and siliciclastic input. Based on TE redox proxies, the paleoenvironment in the Bächental basin during deposition of Units 1 and 3 was characterized by mainly suboxic conditions interrupted by short-term episodes of more intensely reducing conditions. This corresponds well to redox interpretations based on sedimentologic and organic geochemical parameters.

6.3 TE redox proxies in Unit 2 of the Sachrang Member

Black and finely laminated strata of Unit 2 comprising the middle part of the Sachrang Member show high TOC (up to 12.9 %) and HI values (ca. 580-690 mg HC/g TOC; Neumeister et al., 2015). According to organic geochemical (Pr/Ph, GI, hopane isomerization ratio, 4-methylsteranes) and bulk geochemical (TOC-Fe-S) proxies, Subunit 2a accumulated in a strongly reducing, mainly Fe-limited stagnant basinal setting. Intense anoxia was reinforced by a salinity-stratified water column during a period of relative sea-level lowstand. During deposition of Subunit 2b, infrequently occurring turbidity currents served to transiently mix bottom waters and disrupt water-column stratification, although anoxic conditions continued to prevail in the sediment (Figure 2; Neumeister et al., 2015).

Redox-sensitive (Mo, U, and V) as well as bio-sensitive (Cu and Ni) TEs show peak concentrations in Unit 2 (Figures 4A-E, 6). None of the investigated TEs display significant covariation with Al concentrations, and most samples are enriched in TEs distinctly above lithogenous values, suggesting a dominant seawater source (Figures 3A-E, 4A-E). This is confirmed by positive TE-TOC covariation, indicating a chemically controlled TE enrichment process connected to OM accumulation (Figures 3F-J, 6). Hence, availability and preservation of OM were the limiting factors for TE removal to the sediment. The observed TE-TOC correlations are commonly associated with depositional environments characterized by anoxic, but non-euxinic, conditions (Algeo and Maynard, 2004; Tribovillard et al., 2006). The existence of anoxia during deposition of Unit 2 is also suggested by Mo_{EF}/U_{EF} ratios in the lower part of Subunit 2a (Figure 5A; cf. Algeo and Tribovillard, 2009). Low amounts of diagenetic Mn-rich carbonates in Unit 2 (Figure 6; Neumeister et al., 2015) additionally confirm the dominance of strongly reducing conditions as the precipitation of Mn-carbonates is inhibited in fully anoxic environments (Calvert and Pedersen, 1996). Although water-column stratification collapsed during deposition of Subunit 2b due to the episodic occurrence of fine-grained carbonate turbidites (Neumeister et al., 2015), the concurrent trends of TE concentrations and TOC content confirm the persistence of anoxic conditions within the sediment. These redox interpretations are supported by the excellent correspondence of inorganic and organic geochemical proxies (Figure 6; cf. Neumeister et al., 2015).

The occurrence of a salinity-stratified water column induced stagnant and continuously anoxic conditions during deposition of Subunit 2a (Neumeister et al., 2015). In such basinal settings, the ratio of Mo vs. TOC (Mo/TOC) is applicable as a proxy for paleohydrographic restriction (Algeo and Lyons, 2006). The utility of this proxy is based on the continuous removal of Mo to the sediment without adequate resupply by deepwater renewal, causing Mo depletion in the water column. This condition results in low authigenic Mo uptake rates and, hence, low sediment Mo/TOC ratios, despite intensely reducing deepwater conditions (Algeo and Lyons, 2006). In Subunit 2a, low Mo/TOC ratios (<2.4) confirm strong deepwater restriction during its deposition. Furthermore, Mo/TOC ratios show a gradual decline upsection from relative peak values at two stratigraphic levels (grey arrows in Figure 5B), implying multiple intervals of progressive depletion of Mo in stagnant bottom waters (cf. Algeo and Lyons, 2006).

The detailed comparison of vertical trends of organic geochemical proxies (Pr/Ph, GI) and TE concentrations reveals that Pr/Ph ratios of samples with maximum TOC contents show an exceptional behavior. Generally Pr/Ph ratios and GI values are expected to display opposing vertical trends, as seen in Units 1 and 3, because elevated salinity of bottom waters (higher GI) is commonly associated with a stratified water column and more intense reducing conditions (lower Pr/Ph ratio). However, Pr/Ph ratios exhibit significant positive covariation with GI, TE concentrations, and TOC contents in Unit 2 (Figure 6). Pr/Ph values typically <1 confirm the predominance of anoxic conditions during deposition of Subunit 2a. However, the samples characterized by peak values for TOC and GI (e.g., BT 25, 13.39 m) also show slightly elevated Pr/Ph ratios, suggesting a shift to less reducing conditions. We propose that increased values for Pr/Ph ratios were caused by elevated productivity of planktonic and algal organisms in surface waters and/or different pathways of OM transport to the sediment that resulted in a relative increase of Pr. This is consistent with a suggested flourishing of marine algae and bacterioplankton during deposition of the lower part of Subunit 2a (incl. BT 25, 13.39 m) comprising the time interval of the T-OAE (Neumeister et al., 2015). Hence, Pr/Ph ratios signal a flourishing of bioproductivity in parts of Unit 2.

To summarize, TE uptake during deposition of Unit 2 was exclusively associated with OM accumulation, a relationship characteristic of anoxic facies. This is consistent with a stagnant basinal setting as confirmed by bulk geochemical and organic geochemical proxies. Abnormally high Pr/Ph ratios that are found in intervals characterized by high TE concentrations, peak OM preservation, and elevated bottom-water salinity reflect time periods with enhanced bioproductivity.

7. Conclusions

The interpretation of redox proxies based on bulk geochemical parameters, biomarker data as well as TE concentrations and concentration ratios results in a consistent stratigraphic

redox trend for Bächental section. TE compositions of OM-poor samples from the Scheibelberg Formation, the Upper Allgäu Formation and the debrite layer (Sachrang Member) solely derive from lithogenous sources consistent with oxic depositional conditions.

Whereas illite is the only clay mineral in OM-poor rocks of the Scheibelberg and Upper Allgäu formations, smectite, potentially connected with intense volcanic activity in the course of LIP eruptions and/or the breakup of the Alpine Atlantic Ocean, is the dominant clay mineral during the time period of OM accumulation in the Bächental basin. However, the abrupt changes in clay mineralogy at the base and top of the Sachrang Member, respectively, are largely unrelated to TE concentrations in the siliciclastic fraction of the samples. Inorganic geochemical proxies suggest suboxic conditions during deposition of Units 1 and 3. Enrichment of TEs was connected to siliciclastic input (Mo, U, V, Cu, Ni) and potentially to precipitation of diagenetic Mn-rich carbonates (Mo, V) and adsorption onto OM (Cu, Ni).

The occurrence of linear TE-TOC covariations and elevated values for Mo_{EF}/U_{EF} ratio suggest the predominance of anoxic to euxinic conditions during deposition of Subunits 2a and 2b, with OM representing the limiting factor for TE accumulation. In Subunit 2a, low Mo/TOC ratios correspond to strong deepwater restriction and intense anoxia. Pr/Ph ratios are controlled by prevailing redox conditions and bioproductivity. Thus, the comparison of vertical trends of geochemical redox proxies provides a means to detect intervals characterized by elevated surface-water productivity. Accordingly, a flourishing of marine algae and bacterioplankton contributed to the significant TOC increase at the base of Subunit 2a corresponding to the time-equivalent occurrence of OM-rich deposits worldwide connected to the T-OAE.

Acknowledgments

We gratefully thank family Albrecht (Tiroler Steinöl®) who operate the Bächental open pit for their technical support during sampling. Research by TJA is supported by the Sedimentary Geology and Paleobiology program of the U.S. National Science Foundation, the NASA Exobiology program, and the China University of Geosciences-Wuhan (SKL-GPMR program GPMR201301, and SKL-BGEG program BGL201407).

References

Achterberg, E.P., Van Den Berg, C.M.G., Boussemart, M. and Davison, W., 1997. Speciation and cycling of trace metals in Esthwaite Water: a productive English lake with seasonal deep-water anoxia. Geochimica et Cosmochimica Acta, 61, 5233-5253. http://dx.doi.org/10.1016/S0016-7037(97)00316-5

Adelson, J.M., Helz, G.R. and Miller, C.V., 2001. Reconstructing the rise of recent coastal anoxia; molybdenum in Chesapeake Bay sediments. Geochimica et Cosmochimica Acta, 65, 237-252. http://dx.doi.org/10.1016/S0016-7037(00)00539-1

Algeo, T.J. and Maynard, J.B., 2004. Trace-element behaviour and redox facies in core shales of Upper Pennsylvanian Kansas-type cyclothems. Chemical Geology, 206, 289-318. http://dx.doi.org/10.1016/j.chemgeo.2003.12.009

Algeo, T.J. and Maynard, J.B., 2008. Trace-metal covariation as a guide to water-mass conditions in ancient anoxic marine environments. Geosphere, 4(5), 872-887. http://dx.doi.org/10.1130/GES00174.1

Algeo, T. J. and Lyons, T.W., 2006. Mo-total organic carbon covariation in modern anoxic marine environments: Implications for analysis of paleoredox and paleohydrographic conditions. Paleoceanography, 21, PA1016. http://dx.doi.org/10.1029/2004PA001112

Algeo, T. J., and Rowe, H., 2012. Paleoceanographic applications of trace-metal concentration data. Chemical Geology, 324, 6-18. doi:10.1016/j.chemgeo.2011.09.002

Algeo, T.J. and Tribovillard, N., 2009. Environmental analysis of paleoceanographic systems based on molybdenum-uranium covariation. Chemical Geology, 268, 211-225. http://dx.doi.org/10.1016/j.chemgeo.2009.09.001

Berner, R.A., 1981. A new geochemical classification of sedimentary environments. Journal of Sedimentary Petrology, 51, 59-365. http://dx.doi.org/10.1306/212F7C7F-2B24-11D7-8648000102C1865D

Bernoulli, D. and Jenkyns, H.C., 1974. Alpine, Mediterranean and Central Atlantic Mesozoic facies in relation to the early evolution of the Tethys. In: R.H. Dott and R.W. Shaver (eds.), Modern and Ancient Geosynclinal Sedimentation, a Symposium. Special Publication of the Society of economic Paleontologists and Mineralogists, 19, 129-160.

Brandner, R., 2011. In: Geologie des Achenseegebiets. Tagungsband der Arbeitstagung der Geologischen Bundesanstalt, Wien, 220-224.

Breck, W.G., 1974. Redox levels in the sea. In: E.D. Goldberg (eds.), The Sea, vol. 5. Wiley, New York, pp. 153-179.

Breit, G.N. and Wanty, R.B., 1991. Vanadium accumulation in carbonaceous rocks: a review of geochemical controls during deposition and diagenesis. Chemical Geology, 91, 83-97. http://dx.doi.org/10.1016/0009-2541(91)90083-4

Brumsack, H.J., 1986. The inorganic geochemistry of Cretaceous black shales (DSDP Leg 41) in comparison to modern upwelling sediments from the Gulf of California. In: C.P. Summerhayes and N.J. Shackleton (eds.), North Atlantic Palaeoceanography. Geological Society London Special Publications, 21, pp. 447-462. http://dx.doi.org/10.1144/GSL.SP.1986.021.01.30

Brumsack, H.J., 1989. Geochemistry of recent TOC-rich sediments from the Gulf of California and the Black Sea. International Journal of Earth Sciences (formerly Geologische Rundschau), 78, 851-882. http://dx.doi.org/10.1007/BF01829327

Brumsack, H.J., 2006. The trace metal content of recent organic carbon-rich sediments: implications for Cretaceous black shale formation. Palaeogeography Palaeoclimatology Palaeoecology, 232, 344-361. http://dx.doi.org/10.1016/j.palaeo.2005.05.011

Calvert, S.E. and Pedersen, T.F., 1996. Sedimentary geochemistry of manganese: implications for the environment of formation of manganiferous black shales. Economic Geology,

91, 36-47. http://dx.doi.org/10.2113/gsecongeo.91.1.36

Calvert, S.E. and Pedersen, T.F., 2007. Elemental proxies for palaeoclimatic and palaeoceanographic variability in marine sediments: interpretation and application. In: C. Hillaire-Marcel and A. de Vernal (eds.), Paleoceanography of the Late Cenozoic. Part 1. Methods in Late Paleoceanography. Elsevier, New York, pp. 567-644. http://dx.doi.org/10.1016/S1572-5480(07)01019-6

Chen, J.H., Edwards, R.L. and Wasserburg, G.J., 1986. ^{238}U, ^{234}U and ^{232}Th in seawater. Earth and Planetary Science Letters, 80, 241-251. http://dx.doi.org/10.1016/0012-821X(86)90108-1

Cohen, A.S., Coe, A.L., Harding, S.M. and Schwark, L., 2004. Osmium isotope evidence for the regulation of atmospheric CO_2 by continental weathering. Geology, 32, 157-160. http://dx.doi.org/10.1130/G20158.1

Collier, R.W. and Edmond, J.M., 1983. Plankton composition and trace element fluxes from the surface ocean. In: C.S. Wong, E. Boyle, K.W. Bruland, J.D. Burton and E.D. Goldberg (eds.), Trace Metals in Seawater, NATO Conference Series IV-9. Plenum Press, New York, pp. 789-809.

Dean, W.E., Piper, D.Z. and Peterson, L.C., 1999. Molybdenum accumulation in Cariaco basin sediment over the past 24 k. y.: A record of water-column anoxia and climate. Geology, 27, 507-510. http://dx.doi.org/10.1130/0091-7613(1999)027<0507:MAICBS>2.3.CO;2

Didyk, B.M., Simoneit, B.R.T., Brassell, S.C. and Eglinton, G., 1978. Organic geochemical indicators of palaeoenvironmental conditions of sedimentation. Nature, 272, 216-222. http://dx.doi.org/10.1038/272216a0

Ebli, O., 1991 mit Beiträgen von I. Draxler, P. Klein, L.A. Kodina, H. Lobitzer and B. Schwaighofer. Fazies, Paläontologie und organische Geochemie der Sachranger Schiefer (Untertoarcium) im Mittelabschnitt der Nördlichen Kalkalpen zwischen Isar und Saalach. Jahrbuch der Geologischen Bundesanstalt, 134/1, 5-14.

Ebli, O., Vetö, I., Lobitzer, H., Sajgò, C., Demény, A. and Hetényi, M., 1998. Primary productivity and early diagenesis in the Toarcian Tethys on the example of the Mn rich black shales of the Sachrang Formation, Northern Calcareous Alps. Organic Geochemistry, 29, 1635-47. http://dx.doi.org/10.1016/S0146-6380(98)00069-2

Emerson, S.R. and Huested, S.S., 1991. Ocean anoxia and the concentration of molybdenum and vanadium in seawater. Marine Chemistry, 34, 177-196. http://dx.doi.org/10.1016/0304-4203(91)90002-E

Encarnación, J., Fleming, T.H., Elliot, D.H. and Eales, H.V., 1996. Synchronous emplacement of Ferrar and Karoo dolerites and the early breakup of Gondwana. Geology, 24, 535-538. http://dx.doi.org/10.1130/0091-7613(1996)024<0535:SEOFAK>2.3.CO;2

Frimmel, A., Oschmann, W. and Schwark, L., 2004. Chemostratigraphy of the Posidonia Shale, SW Germany I. Influence of sea-level variation on organic facies evolution. Chemical Geology, 206, 199-230. http://dx.doi.org/10.1016/j.chemgeo.2003.12.007

Frisch, W. and Gawlick, H.-J., 2003. The nappe structure of the central Northern Calcareous Alps and its disintegration during Miocene tectonic extrusion – a contribution to understanding the orogenic evolution of the Eastern Alps. International Journal of Earth Sciences (formerly Geologische Rundschau), 92, 712-727. http://dx.doi.org/10.1007/s00531-003-0357-4

Fu, J.G., Sheng, P., Peng, S.C., Brassell, S.C. and Eglington, G., 1986. Pecularities of salt lake sediments as potential source rocks in China. Organic Geochemistry 10, 119-127. doi:10.1016/0146-6380(86)90015-X

Gawlick, H.-J., Missoni, S., Schlagintweit, F., Suzuki, H., Frisch, W., Krystyn, L., Blau, J. and Lein, R., 2009. Jurassic Tectonostratigraphy of the Austroalpine Domain. Journal of Alpine Geology, 50, 1-152.

Helz, G.R., Miller, C.V., Charnock, J.M., Mosselmans, J.F.W., Pattrick, R.A.D., Garner, C.D. and Vaughan, D.J., 1996. Mechanism of molybdenum removal from the sea and its concentration in black shales: EXAFS evidence. Geochimica et Cosmochimica Acta, 60, 3631–3642. http://dx.doi.org/10.1016/0016-7037(96)00195-0

Ho, T.Y., Quigg, A., Finkel, Z.V., Milligan, A.J., Wyman, K., Falkowski, P.G. and Morel, F.M., 2003. The elemental composition of some marine phytoplankton. Journal of Phycology, 39, 1145-1159. http://dx.doi.org/10.1111/j.0022-3646.2003.03-090.x

Holland, H.D., 1984. The Chemical Evolution of the Atmosphere an Oceans. Princeton University Press, Princeton, N.Y., 582 pp.

Huerta-Diaz, M.A. and Morse, J.W., 1992. Pyritisation of trace metals in anoxic marine sediments. Geochimica et Cosmochimica Acta, 56, 2681-2702. http://dx.doi.org/10.1016/0016-7037(92)90353-K

Ikeda, M. and Hori, R.S., 2014. Effects of Karoo-Ferrar volcanism and astronomical cycles on the Toarcian Anoxic Events (Early Jurassic). Palaeogeography, Palaeoclimatology, Palaeoecology, 410, 134-142. http://dx.doi.org/10.1016/j.palaeo.2014.05.026

Jenkyns, H.C., 1985. The Early Toarcian and Cenomanian–Turonian anoxic events in Europe: comparisons and contrasts. International Journal of Earth Sciences (formerly Geologische Rundschau), 74, 505-518. http://dx.doi.org/10.1007/BF01821208

Jenkyns, H.C., 1988. The Early Toarcian (Jurassic) anoxic event: stratigraphic, sedimentary, and geochemical evidence. American Journal of Science, 288, 101-151. http://dx.doi.org/10.2475/ajs.288.2.101

Jenkyns, H.C., Jones, C.E., Gröcke, D.R., Hesselbo, S.P. and Parkinson, D.N., 2002. Chemostratigraphy of the Jurassic System: applications, limitations and implications for palaeoceanography. Journal of the Geological Society of London, 159, 351-378. http://dx.doi.org/10.1144/0016-764901-130

Jenkyns, H.C., 2003. Evidence for rapid climate change in the Mesozoic–Palaeogene greenhouse world. Philosophical Transactions of the Royal Society of London, 361 A, 1885-1916. http://dx.doi.org/10.1098/rsta.2003.1240

Jenkyns, H.C., 2010. The geochemistry of oceanic anoxic events. Geochemistry Geophysics Geosystems, 11, Q03004.

http://dx.doi.org/10.1029/2009GC002788.

Klebelsberg, R.v., 1935. Geologie von Tirol. Gebrüder Borntraeger, Berlin, 872 pp.

Kodina, L.A., Bogatecheva, M.P. and Lobitzer, H., 1988. An anorganic geochemical study of Austrian bituminous rocks. Jahrbuch der Geologischen Bundesanstalt, 131, 291-300.

Kogel, J.E. and Lewis, S.A., 2001. Baseline studies of the clay minerals society source clays: Chemical analysis by inductively coupled plasma-mass spectroscopy (ICP-MS). Clays and Clay Minerals, 49(5), 387-392.

Lewan, M.D. and Maynard, J.B., 1982. Factors controlling enrichment of vanadium and nickel in the bitumen of organic sedimentary rocks. Geochimica et Cosmochimica Acta, 46, 2547-2560. http://dx.doi.org/10.1016/0016-7037(82)90377-5

Littke, R., Rotzal, H., Leythaeuser, D. and Baker, D.R., 1991. Organic facies and maturity of Lower Toarcian Posidonia Shale in Southern Germany (Schwäbische Alb). Erdöl & Kohle Erdgas Petrochemie/Hydrocarbon Technology, 44, 407-414.

Lyle, M., 1976. Estimation of hydrothermal manganese input to the oceans. Geology, 4, 733-736. http://dx.doi.org/10.1130/0091-7613(1976)4<733:EOHMIT>2.0.CO;2

Martin, J.H. and Meybeck, M., 1979. Elemental mass-balance of material carried by major world rivers. Marine Chemistry, 7, 173-206. http://dx.doi.org/10.1016/0304-4203(79)90039-2

Marzoli, A., Renne, P.R., Piccirillo, E.M., Ernesto, M., Bellieni, G. and De Min, A., 1999. Extensive 200 million-year-old continental flood basalts of the central Atlantic magmatic province. Science, 284, 616-618. http://dx.doi.org/10.1126/science.284.5414.616

McLennan, S.M., 2001. Relationships between the trace element composition of sedimentary rocks and upper continental crust. Geochemistry Geophysics Geosystems, 2, paper # 2000GC000109. http://dx.doi.org/10.1029/2000GC000109

Minor, D.R. and Mukasa, S.B., 1997. Zircon U-Pb and hornblende ^{40}Ar-^{39}Ar ages for the Dufek layered mafic intrusion, Antarctica: Implications for the age of the Ferrar large igneous province. Geochimica et Cosmochimica Acta, 61, 2497-2504. http://dx.doi.org/10.1016/S0016-7037(97)00098-7

Morford, J.L. and Emerson, S., 1999. The geochemistry of redox sensitive trace metals in sediments. Geochimica et Cosmochimica Acta, 63, 1735-1750. http://dx.doi.org/10.1016/S0016-7037(99)00126-X

Morford, J.L., Russell, A.D. and Emerson, S., 2001. Trace metal evidence for changes in the redox environment associated with the transition from terrigenous clay to diatomaceous sediments, Saanich Inlet, BC. Marine Geology, 174, 355-369. http://dx.doi.org/10.1016/S0025-3227(00)00160-2

Morford, J.L., Emerson, S.R., Breckel, E.J. and Kim, S.H., 2005. Diagenesis of oxyanions (V, U, Re, and Mo) in pore waters and sediments from a continental margin. Geochimica et Cosmochimica Acta, 69, 5021-5032. http://dx.doi.org/10.1016/j.gca.2005.05.015

Morse, J.W. and Luther III, G.W., 1999. Chemical influences on trace metal-sulfide interactions in anoxic sediments. Geochimica et Cosmochimica Acta, 63, 3373-3378. http://dx.doi.org/10.1016/S0016-7037(99)00258-6

Naimo, D., Adamo, P., Imperato, M. and Stanzione, D., 2005. Mineralogy and geochemistry of a marine sequence, Gulf of Salerno, Italy. Quaternary International, 140-141, 53-63. http://dx.doi.org/10.1016/j.quaint.2005.05.004

Nameroff, T.J., Calvert, S.E. and Murray, J.W., 2004. Glacial-interglacial variability in the eastern tropical North Pacific oxygen minimum zone recorded by redox-sensitive trace metals. Paleoceanography, 19, PA1010. http://dx.doi.org/10.1029/2003PA000912.

Neumeister, S., Gratzer, R., Algeo, T.J., Bechtel, A., Gawlick, H.-J., Newton, R.J. and Sachsenhofer, R.F., 2015. Oceanic response to Pliensbachian and Toarcian magmatic events: Implications from an organic-rich basinal succession in the NW Tethys. Global and Planetary Change, 126, 62-83. http://dx.doi.org/10.1016/j.gloplacha.2015.01.007

Pálfy, J. and Smith, P.L., 2000. Synchrony between Early Jurassic extinction, oceanic anoxic event, and the Karoo–Ferrar flood basalt volcanism. Geology, 28, 747-750. http://dx.doi.org/10.1130/0091-7613(2000)28<747:SBEJEO>2.0.CO;2

Parrish, J.T., 1993. Climate of the supercontinent Pangaea. Journal of Geology, 101, 215-233.

Parrish, J.T. and Curtis, R.L., 1982. Atmospheric circulation, upwelling, and organic-rich rocks in the Mesozoic and Cenozoic areas. Palaeogeography, Palaeoclimatology, Palaeoecology, 40, 31-66. http://dx.doi.org/10.1016/0031-0182(82)90084-0

Pearce, C.R., Cohen, A.S., Coe, A.L. and Burton, K.W., 2008. Molybdenum isotope evidence for global ocean anoxia coupled with perturbations to the carbon cycle during the Early Jurassic. Geology, 36, 231-234. http://dx.doi.org/10.1130/G24446A.1

Perkins, R.B., Piper, D.Z. and Mason, C.E., 2008. Trace-element budgets in the Ohio-Sunbury shales of Kentucky: constraints on ocean circulation and primary productivity in the Devonian-Mississippian Appalachian Basin. Palaeogeography Palaeoclimatology Palaeoecology, 265, 14-29. http://dx.doi.org/10.1016/j.palaeo.2008.04.012

Piper, D.Z. and Perkins, R.B., 2004. A modern vs. Permian black shale – the hydrography, primary productivity, and water-column chemistry of deposition. Chemical Geology, 206, 177-197. http://dx.doi.org/10.1016/j.chemgeo.2003.12.006

Piper, D.Z., Perkins, R.B. and Rowe, H.D., 2007. Rare-earth elements in the Permian Phosphoria Formation: paleo proxies of ocean geochemistry. Deep-Sea Research, 54, 1396-1413. http://dx.doi.org/10.1016/j.dsr2.2007.04.012

Piper, D.Z. and Calvert, S.E., 2009. A marine biogeochemical perspective on black shale deposition. Earth Science Reviews, 95, 63-96. http://dx.doi.org/10.1016/j.dsr2.2007.04.012

Pratt, L.M. and Davis, C.L., 1992. Intertwined fates of metals, sulphur, and organic carbon in black shales. In: Pratt et al. (Eds.), Geochemistry of Organic Matter in Sediments and Sedimentary Rocks. SEPM Short Course, 27, 1-27.

Praus, M. and Riegel, W., 1989. Evidence from phytoplanktonic associations for causes of black shale formation in epiconti-

nental seas. Neues Jahrbuch für Geologie und Paläontologie, Monatshefte, 11, 671-682.

Ratschbacher, L., Dingeldey, C., Miller, C., Hacker, B.R. and McWilliams, M.O., 2004. Formation, subduction, and exhumation of Penninic oceanic crust in the Eastern Alps: time constraints from $^{40}Ar/^{39}Ar$ geochronology. Tectonophysics, 394, 155-170. http://dx.doi.org/10.1016/j.tecto.2004.08.003

Rex, R.W. and Goldberg, E.D., 1958. Quartz contents of pelagic sediments in the Pacific Ocean. Tellus, 10, 153-159.

Robl, T.L. and Barron, L.S., 1987. The geochemistry of Devonian black shales in central Kentucky and its relationship to interbasinal correlation and depositional environment. In: N.J. McMillan et al. (eds.), Devonian of the World, 2, Sedimentation. Mem. of the Canadian Society of Petroleum Geologists, 14, pp. 377-392.

Röhl, H.J., Schmid-Röhl, A., Oschmann, W., Frimmel, A. and Schwark, L., 2001. The Posidonia Shale (Lower Toarcian) of SW-Germany: an oxygen-depleted ecosystem controlled by sea level and palaeoclimate. Palaeogeography, Palaeoclimatology, Palaeoecology, 165, 27-52. http://dx.doi.org/10.1016/S0031-0182(00)00152-8

Sælen, G., Doyle, P. and Talbot, M.R., 1996. Stable-isotope analysis of belemnite rostra from the Whitby Mudstone Fm., England: Surface water conditions during deposition of a marine black shale. Palaios, 11, 97-117. http://dx.doi.org/10.2307/3514466

Savrda, C.E. and Bottjer, D.J., 1991. Oxygen-related biofacies in marine strata: an overview and update. In: R.V. Tyson and T.H. Pearson (eds.), Modern and Ancient Continental Shelf Anoxia. Geological Society London Special Publications, 58, pp. 201-219.

Schlager, W. and Schöllnberger, W., 1973. Das Prinzip stratigraphischer Wenden in der Schichtfolge der Nördlichen -Kalkalpen. Mitteilungen der Geologischen Gesellschaft Wien, 66, 166-193.

Schmid-Röhl, A., Röhl, H.-J., Oschmann, W., Frimmel, A. and Schwark, L., 2002. Palaeoenvironmental reconstruction of Lower Toarcian epicontinental black shales (Posidonia Shale, SW Germany): global versus regional control. Geobios, 35, 13-20. http://dx.doi.org/10.1016/S0016-6995(02)00005-0

Schwark, L., Vliex, M. and Schaeffer, P., 1998. Geochemical characterization of Malm Zeta laminated carbonates from the Franconian Alb, SW Germany (II). Organic Geochemistry, 29, 1921-1952. doi:10.1016/S0146-6380(98)00192-2

Scott, C., Lyons, T. W., Bekker, A., Shen, Y., Poulton, S. W., Chu, X., and Anbar, A. D., 2008. Tracing the stepwise oxygenation of the Proterozoic ocean. Nature, 452(7186), 456-459. doi:10.1038/nature06811

Sell, B., Ovtcharova, M., Guex, J., Bartolini, A., Jourdan, F., Spangenberg, J.E., Vicente, J.-C. and Schaltegger, U., 2014. Evaluating the temporal link between the Karoo LIP and climatic-biologic events of the Toarcian Stage with high-precision U-Pb geochronology. Earth and Planetary Science Letters, 408, 48-56. http://dx.doi.org/10.1016/j.epsl.2014.10.008

Sinninghe Damsté, J.S., van Duin, A.C.T., Hollander, D., Kohnen, M.E.L. and de Leeuw, J.W., 1995. Early diagenesis of bacteriohopanepolyol derivatives: Formation of fossil homohopanoids. Geochimica et Cosmochimica Acta 59, 5141-5156. doi:10.1016/0016-7037(95)00338-X

Spieler, A. and Brandner, R., 1989. Vom jurassischen Pull-Apart Becken zur Westüberschiebung der Achentaler Schubmasse (Tirol, Österreich). Geologisch-Paläontologische Mitteilungen Innsbruck, 16, 191-194.

Suan, G., Schlögl, J. and Mattioli, E., 2016. Bio- and chemostratigraphy of the Toarcian organic-rich deposits of some key successions of the Alpine Tethys. Newsletters on Stratigraphy, 44 (2016). http://dx.doi.org/10.1127/nos/2016/0078

Svensen, H., Planke, S., Chevalier, L., Malthe-Sørensen, A., Corfu, F. and Jamveit, B., 2007. Hydrothermal venting of greenhouse gases triggering Early Jurassic global warming. Earth and Planetary Science Letters, 256, 554-566. http://dx.doi.org/10.1016/j.epsl.2007.02.013

Svensen, H., Corfu, F., Polteau, S., Hammer, Ø. and Planke, S., 2012. Rapid magma emplacement in the Karoo Large Igneous Province. Earth and Planetary Science Letters, 325–326, 1-9. http://dx.doi.org/10.1016/j.epsl.2012.01.015

Taylor, S.R. and McLennan, S.M., 1985. The Continental Crust, its Composition and Evolution. Blackwell Scientific, Oxford. 312 pp.

ten Haven, H.L., de Leeuw, J.W. and Schenk, P.A., 1985. Organic geochemical studies of a Messinian evaporitic basin, northern Appenines (Italy): Hydrocarbon biological markers for a hypersaline environment. Geochimica et Cosmochimica Acta 49, 2181-2191. doi:10.1016/0016-7037(85)90075-4

ten Haven, H.L., de Leeuw, J.W., Rullkötter, J. and Sinninghe Damsté, J.S., 1987. Restricted utility of the pristane/phytane ratio as a palaeoenvironmental indicator. Nature 330, 641-643. doi:10.1038/330641a0

Thomson, J., Higgs, N.C., Croudace, I.W., Colley, S. and Hydes, D.J., 1993. Redox zonation of elements at an oxic/post-oxic boundary in deep-sea sediments. Geochimica et Cosmochimica Acta, 57(3), 579-595. http://dx.doi.org/10.1016/0016-7037(93)90369-8

Tollmann, A., 1976. Analyse des klassischen nordalpinen Mesozoikums. Stratigraphie, Fauna und Fazies der Nördlichen Kalkalpen. Deuticke, Wien, 580 pp.

Tribovillard, N., Algeo, T.J., Lyons, T. and Riboulleau, A., 2006. Trace metals as paleoredox and paleoproductivity proxies: An update. Chemical Geology, 232, 12-32. http://dx.doi.org/10.1016/j.chemgeo.2006.02.012

Von Damm, K.L., 1990. Seafloor hydrothermal activity: Black smoker chemistry and chimneys. Annual Review of Earth and Planetary Sciences, 18, 173-204. http://dx.doi.org/10.1146/annurev.ea.18.050190.001133

Wedepohl, K.H., 1971. Environmental influences on the chemical composition of shales and clays. Physics and Chemistry of the Earth, 8, 305-333. http://dx.doi.org/10.1016/0079-1946(71)90020-6

Wedepohl, K.H., 1995. The composition of the continental

crust. Geochimica et Cosmochimica Acta, 59, 1217-1232. http://dx.doi.org/10.1016/0016-7037(95)00038-2

Weissert, H., 2000. Deciphering methane's fingerprint. Nature, 406, 356-357. http://dx.doi.org/10.1038/35019230

Whiteside, J.H., Olsen, P.E., Kent, D.V., Fowell, S.J. and Et-Touhami, M., 2007. Synchrony between the Central Atlantic magmatic province and the Triassic-Jurassic mass extinction event? Palaeogeography, Palaeoclimatology, Palaeoecology, 244, 345-367. http://dx.doi.org/10.1016/j.palaeo.2006.06.035

Wignall, P.B., 1994. Black Shales. Clarendon Press, Oxford, 127 pp.

Yarincik, K.M., Murray, R.W. and Peterson, L.C., 2000. Climatically sensitive eolian and hemiplegic deposition in the Cariaco Basin, Venezuela, over the past 578,000 years: results from Al/Ti and K/Al. Paleoceanography, 15, 210-228. http://dx.doi.org/10.1029/1999PA900048

Zheng, Y., Anderson, R.F., van Geen, A. and Fleisheir, M.Q., 2002. Preservation of non-lithogenic particulate uranium in marine sediment. Geochimica et Cosmochimica Acta, 66, 3085-3092. http://dx.doi.org/10.1016/S0016-7037(01)00632-9

Received: 07. January 2015
Accepted: 24 March2016

Stefan NEUMEISTER[1) *)], Thomas J. ALGEO[2)], Achim BECHTEL[1)], Hans-Jürgen GAWLICK[1)], Reinhard GRATZER[1)] & Reinhard F. SACHSENHOFER[1)]

[1)] Department of Applied Geosciences and Geophysics, Montanuniversitaet Leoben, Peter-Tunner-Str. 5, A-8700 Leoben, Austria;

[2)] Department of Geology, University of Cincinnati, Cincinnati, OH 45221, USA;

[*)] Corresponding author: st.neumeister@hotmail.com